Advances in computational photochemistry and chemiluminescence of biological and nanotechnological molecules

Daniel Roca-Sanjuán,*[a] Antonio Francés-Monerris,[a] Ignacio Fdez. Galván,[b,c] Pooria Farahani,[d] Roland Lindh*[b,c] and Ya-Jun Liu*[e]

DOI: 10.1039/9781782626954-00016

Recent advances (2014–2015) in computational photochemistry and chemiluminescence derive from the development of theory and from the application of state-of-the-art and new methodology to challenging electronic-structure problems. Method developments have mainly focused, first, on the improvement of approximate and cheap methods to provide a better description of non-adiabatic processes, second, on the modification of accurate methods in order to decrease the computation time and, finally, on dynamics approaches able to provide information that can be directly compared with experimental data, such as yields and lifetimes. Applications of the *ab initio* quantum-chemistry methods have given rise to relevant findings in distinct fields of the excited-state chemistry. We briefly summarise, in this chapter, the achievements on photochemical mechanisms and chemically-induced excited-state phenomena of interest in biology and nanotechnology.

1 Introduction

The 2015 was a year of celebration for the scientists doing research on light–matter interaction. The reason is that the UNESCO recognized that year as the *International Year of Light and Light-Based Technologies*.[1] Several events were organized all around the world to disseminate to the society the crucial role of light in science and culture. We (the theoreticians) were not an exception. Special Issues in journals on Computational Chemistry were produced, in which we showed the relevance of Computational Photochemistry to comprehend the light-induced phenomena taking place in living beings and also to design new technologies that use the chemistry of the excited states. See, for example, the special issue Health & Energy from the Sun: A Computational Perspective of the *Theor. Chem. Acc.* journal.

[a]*Instituto de Ciencia Molecular, Universitat de València, P.O. Box 22085, 46071 València, Spain. E-mail: Daniel.Roca@uv.es*
[b]*Department of Chemistry – Ångström, Theoretical Chemistry Programme, Uppsala University, Uppsala, Sweden. E-mail: Roland.Lindh@kemi.uu.se*
[c]*Uppsala Centre for Computational Chemistry – UC_3, Uppsala University, Uppsala, Sweden*
[d]*Departamento de Química Fundamental, Instituto de Química, Universidade de São Paulo, 05588-000 São Paulo, SP, Brazil*
[e]*Key Laboratory of Theoretical and Computational Photochemistry, Ministry of Education, College of Chemistry, Beijing Normal University, Beijing, China. E-mail: yajun.liu@bnu.edu.cn*

A second event made some of us, who study the photochemistry and photophysics of DNA/RNA, celebrate twice the year 2015: the Nobel Prize was awarded jointly to Tomas Lindahl, Paul Modrich and Aziz Sancar *for mechanistic studies of DNA repair*.[2] Nucleic acids are exposed to several sources of potential damage, among them the UV light, reactive oxygen species (ROS), and other exogenous or endogenous molecules able to sensitize polynucleotides. DNA repair is therefore crucial to provide chemical stability for life.

In this chapter, we continue with our biannual contribution to the RSC Photochemistry Specialist Reports.[3–5] We review in this occasion the advances in computational photochemistry in 2014 and 2015. As in the previous volumes, we begin with the methodological developments and then we continue with the applications. Thus, the first section shall review the works about theory. Next, as a tribute to the Nobel Prize on chemistry, we open a full section dedicated to describe advances in the field of DNA/RNA damage and repair. A few selected studies will be described in more detail to show the intimate equilibrium between damage and stability. After that, a section will follow reviewing other photochemical studies of interest in biology and technology. The remaining sections on applications shall be devoted to the chemi- and bioluminescence phenomena and the chemically-induced excited-state processes (so-called photochemistry without light or ''dark photochemistry''). Finally, all the advances in the field will be summarized. As in previous contributions, our goal is not to make an exhaustive account on the methodological developments and applied works, but an overview of the recent trends including illustrative examples.

2 Development of methods and theory

This section is devoted to recent developments with respect to new theory and method developments in the field of photochemistry and non-adiabatic reactions. A survey of the publications in 2014–15 gives a natural subdivision of this section into three categories: method developments, dynamics, and review papers in the field of non-adiabatic chemistry. In the first category we find reports on how to modify density functional theory (DFT) methods to have a correct dimensionality of the conical intersection (CIX), the assessment of approximate methods in describing the CIX, finding CIX in solution, the improved treatment of time dependent (TD)-DFT for Rydberg states, the use of frozen natural orbitals in conjunction with the multi-configurational second order perturbation theory (FNO-CASPT2), and the combination of multi-configurational wave function theory with DFT for ground and excited states. In the second category we will report on methods using local control theory (LCT) to select the product of the interaction between a molecule and light, on how including tunnelling in semi-classical simulations of non-adiabatic reactions, on the use of symmetrical windowing for quantum states in semi-classical techniques, on improved and simple methods for diabatizations, and the use of Smolyak's technique in dynamical simulations. Finally, we would like to attract some attention to

a number of extensive reviews and perspectives published in the field. Below, we will dwell in some details on these different reports. The comments will, however, be short and limited. Once again, our ambition is not to give the full picture, but enough information to incite the interested reader to proceed with a more detailed reading of the work we cite here.

2.1 Method development

In the last decades, CIXs have received very much attention in theoretical photochemistry studies. Once thought to be an anecdotal feature of potential energy surfaces (PESs), CIXs are now known to be almost ubiquitous and are considered fundamental in the description of photophysical and photochemical processes. At a CIX point, two electronic states are degenerate, and the degeneracy is lifted linearly in 2 dimensions in nuclear configuration space, so that the intersection space has $N-2$ dimensions (with N the total number of nuclear degrees of freedom). Not all methods commonly used to study excited states produce the correct dimensionality for CIXs. For example, with regular TDDFT methods, intersections between the reference (ground) state and an excited state have $N-1$ dimensions, *i.e.*, the degeneracy is lifted along a single direction and the intersection is no longer truly ''conical''. This is one of the issues that cripple the use of TDDFT methods for photochemical studies, since it is a fundamental flaw that can have important consequences for dynamics simulations. Li *et al.*[6] proposed a modification to the Tamm-Dancoff approximation to linear-response TDDFT that recovers the correct topology of CIXs (Fig. 1). The modification, named configuration interaction-corrected Tamm-Dancoff approximation (CIC-TDA) is based on including the coupling between the reference state and a single-excitation response state, interpreting the corresponding Slater determinants as if they were wave functions. The authors showed in two examples that this simple correction fixes unphysical double crossings in PESs and does not introduce significant changes far from the CIX.

The ability of other approximate computational methods to correctly describe CIXs was examined by Nikiforov *et al.*[7] They compared two other DFT-based methods (spin-flip TDDFT: SF-TDDFT, state-interaction state-averaged restricted ensemble-referenced Kohn-Sham: SI-SA-REKS), as well as a semiempirical model (orthogonalization model 2/multi-reference configuration interaction, OM2/MRCI), with the reference MRCI including single and double excitations (MRCISD). The comparison was focused on the structures for optimized minimum-energy CIXs and the corresponding branching plane vectors (the two directions along which the degeneracy is lifted) for a set of 12 intersections in 8 compounds. The authors showed that agreement between the structures optimized with the different methods is satisfactory. When comparing the branching planes, care should be taken since the vectors are allowed to rotate without modifying the plane they span; after taking this into account the agreement between the branching planes obtained with the different methods was also very good. The main conclusion was that the

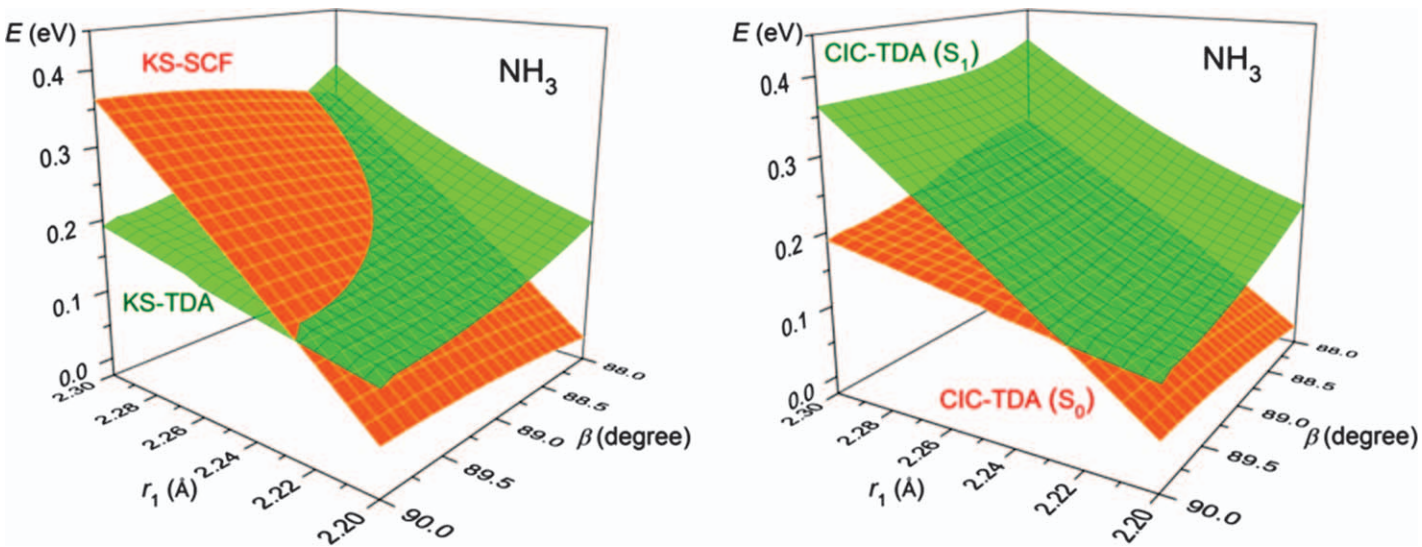

Fig. 1 Potential energy surfaces (PESs) of the two lowest-energy states of NH_3 as calculated by (left) Kohn-Sham (KS)-TDA and (right) CIC-TDA. [Reprinted with permission from *J. Phys. Chem. Lett.*, 2014, **5**, 322. Copyright 2014 American Chemical Society.]

approximate methods tested in the work provide reasonably accurate results, supporting their use for modeling the photochemistry of large organic and biological systems.

The chemical environment (such as a solvent) can have a very significant effect in the mechanisms of photochemical reactions. A useful approximation for understanding these effects is studying how the PESs and CIXs are modified in the presence of a solvent. An added complication is the fact that these reactions typically take place under non-equilibrium conditions, where the reactant is strongly perturbed by the initial excitation. Minezawa[8] proposed a method for optimizing CIXs taking into account these non-equilibrium conditions to some extent. The method is based on SF-TDDFT, reference interaction site model SCF (RISM-SCF) for introducing the solvent effects and linear-response free energy (LRFE) for off-equilibrium solvation. In this formulation a number of solvent coordinates are introduced that affect the electrostatic potential acting on the solute nuclei, and both solute and solvent coordinates are optimized to obtain a free-energy crossing point in solution. This approach was tested for stilbene in acetonitrile and thymine in water. Although the results should be taken with caution, since they cannot represent the real dynamics under strong non-equilibrium conditions, they offer a promising characterization and rationalization of the solvent effects on the CIXs.

The computational treatment of electronic excited states often requires the use of multiconfigurational *ab initio* methods, as single-reference methods like current DFT functionals cannot provide a good enough description. However, the inclusion of dynamical correlation through perturbation theory (as in CASPT2) or through extensive CI expansions (MRCI) can easily become too computationally expensive to be of practical use. There has been some interest in combining the efficiency of DFT techniques with multiconfigurational methods, and Li Manni *et al.*[9] developed a theoretical framework for this called multiconfigurational pair-density functional theory (MC-PDFT). In this method a pragmatic approach is taken to compute the energies: starting from a standard complete-active-space self-consistent field (CASSCF) calculation which captures the fundamental static correlation in the system, the total electron density ρ and the on-top pair density Π are obtained. Then the one-electron energy terms and the electronic Coulomb energy are computed from ρ (or the one-electron density matrix), and an additional term is added from an on-top density functional. Initial on-top density functionals are obtained from simple ''translation'' of common exchange–correlation functionals, giving encouraging results. In this way, double-counting of electron correlation is avoided, since the final energy does not mix wavefunction and DFT terms. The results for excitation energies and potential energy curves significantly improve the CASSCF values, competing with CASPT2, at a negligible additional computational cost. It was also shown that the method has very good performance for ground-state and excited-state charge transfer (Fig. 2).[10]

Within the more standard wavefunction methods, a more pragmatic approach was taken by Segarra-Martí *et al.*[11] In the CASPT2 method, the

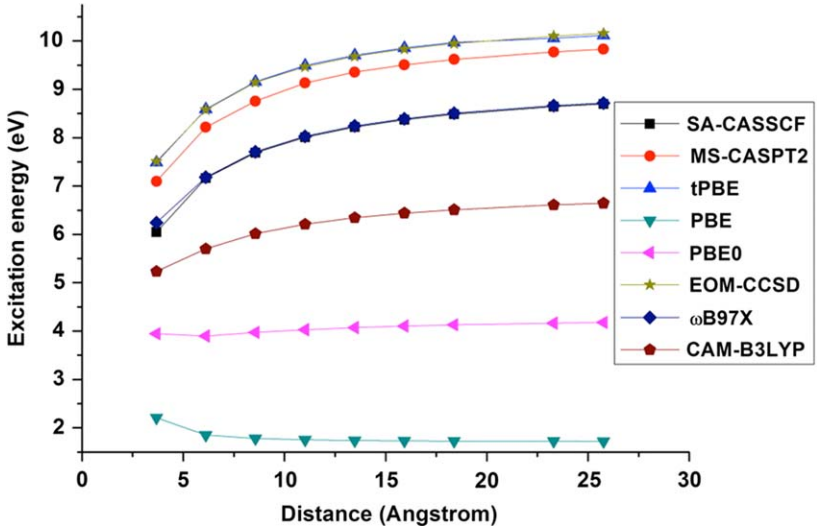

Fig. 2 Charge-transfer excitation energy for $NH_3\cdots HNO_2$. Note that the tPBE (MC-PDFT) curve is almost coincident with equation of motion-coupled cluster with single and double excitations (EOM-CCSD). [Reprinted with permission from *J. Chem. Theory Comput.*, 2015, **11**, 3643. Copyright 2015 American Chemical Society.]

computational cost scales quadratically with the total number of orbitals in the system. This makes calculations of moderately large molecules or with accurate basis sets too expensive for routine use. The frozen natural orbital (FNO-CASPT2) approximation has been proposed based on truncating the virtual orbital space, thus removing the contributions of a fraction of the virtual orbitals to the correlation energy. While this results in significant time savings with a similar accuracy to the untruncated calculation, it suffers from discontinuities in the PES, making it inadequate for geometry optimizations, or PES mapping. The reason for the discontinuities is that the orbitals excluded from the perturbation step are selected with a simple energy criterion and their contribution to the correlation energy is not constant at different molecular geometries. The authors presented a new variation of the method, which selects the orbitals based on their contribution to the correlation energy (as estimated from their contribution to the trace of the one-particle density matrix). They showed that by preserving 97.5–99% of the trace, 40–50% of the virtual orbitals can be removed, three-fold speed-ups can be obtained and the errors in the energy are within 0.1 eV. More importantly, the energy curves with these conditions are sufficiently smooth that they can be used for geometry optimization or for studying photochemical processes (Fig. 3).

A usual problem with TDDFT methods with common local and hybrid functionals is that the excitation energies of Rydberg states are greatly underestimated. This can be traced back to the self-interaction error due to the failure of local exchange approximations to exactly cancel the spurious Coulomb interaction of an electron with itself. As the error affects differently valence and Rydberg orbitals, exchange–correlation

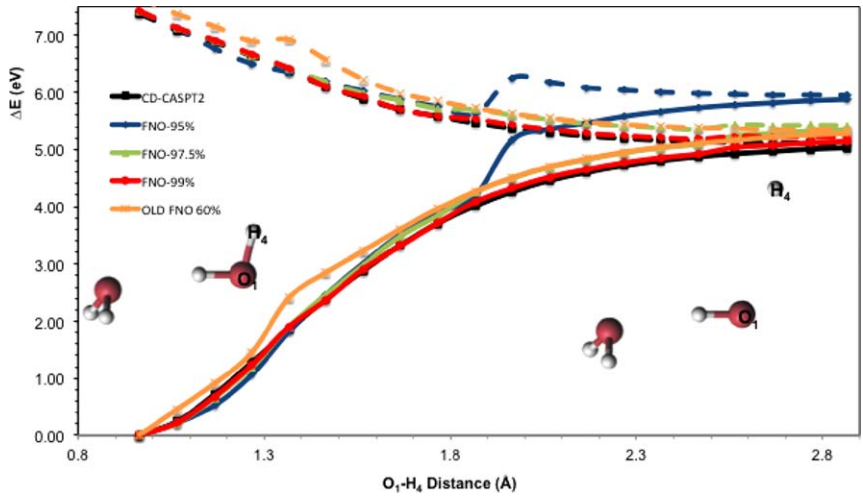

Fig. 3 Photodissociation curves of the water dimer for different truncations of the virtual orbital space with CASPT2. Cholesky decomposition (CD)-CASPT2: no truncation, OLD FNO *x*%: previous implementation with fixed fraction (*x*%) of virtual orbitals retained, FNO-*x*%: new implementation with fraction of density matrix trace (*x*%) retained (variable number of orbitals). [Reprinted with permission from *J. Chem. Theory Comput.*, 2015, **11**, 3772. Copyright 2015 American Chemical Society.]

functionals typically used to describe valence states result in too low-lying Rydberg states. Li and Truhlar[12] suggested that a modification of the exchange functionals in the regions of high reduced density gradient (long distance from the nuclei) can increase the energy of Rydberg orbitals relative to valence orbitals, therefore improving the balance between valence and Rydberg states. They proposed such a modification be applicable, in principle, to any generalized gradient approximation (GGA) functional. Their scheme, named exchange-enhancement-for-large-gradient (XELG), was tested by modifying the PBE0 functional, and shown to diminish the errors in the excitation energies to Rydberg states while having little effect on the valence states.

2.2 Dynamics

The development of methods for dynamics has come a long way since the suggestion by Tully to use the so-called trajectory surface hopping (TSH) approach to acquire ensembles of trajectories which together describe the evolution in time of the total wavefunction during a non-adiabatic process. The alternative approach, more accurate, expensive, and limited to smaller molecular systems—the quantum molecular dynamics (QMD) approach—is still, however, used and of importance.

Below we will describe two reports, one which includes the tunneling effect into, for example, conventional TSH implementations, reducing the length and number of required trajectories to converge the so-called non-reactive probability, and a second one which introduces the model space diabatization (MSD) to wavefunctions including dynamic electron

correlation at the multi-state and multi-configurational level of approximation. The latter is of importance for the QMD and the associated PES fitting and parametrization which is so important for its use and success. With the merge of techniques for simulation of non-adiabatic processes to simulate photo-initiated processes and map out the nature of the subsequent photochemical and photophysical processes, scientists started to ask the question ''Is it possible to control these processes by designing the shape of the radiation pulse?''. Indeed that is possible, different approaches to this have been published and here we will report on the use of local control theory in association with TSH for controlled proton transfer. Finally, much of the basic theory of molecular dynamics is known and understood; however, the time-dependent versions of the Schrödinger and Dirac equations are too complicated to be solved by brute force. As with electron-structure theory, technical and engineering-like solutions to specific computational problems, if addressed correctly, can be a major leap forward in the applicability of specific computational protocols. In electron-structure theory we have witnessed the development of so-called linear-scaling methods, often extremely technical in their nature, as a major advance in the applicability of the methods to much larger systems as compared to before. It is our opinion that the methods of simulations of molecular dynamic processes are going through the very same changes, modifications and improvements. In the future new technique will allow for simulations of a size and accuracy which is beyond what we see today. These changes and improvements are by nature incremental. In this report we will describe two such improvements, which have the potential of being significant steps forward. First, we will describe the symmetrical windowing quasi-classical (SQC) approach to pick up quantum coherence effects in simple classical approaches. Second, we will digest the report on the use of a sparse interpolation algorithm—Smolyak's method—in dynamics simulations, as a tool to explore several different reaction paths without the associated increase in computational expense.

The lack of tunneling effects in semi-classical simulations of Born–Oppenheimer and non-adiabatic reactions has to be considered one of the major drawbacks of semi-classical approaches. In particular, in biochemical systems and reactions, hydrogen and proton transfers are key reactions steps. The correct assessment of reaction rates and quantum yields are of significance, and here the tunneling effects exclusion or inclusion can have significant impact of the qualitative and quantitative accuracy that simulations can bring to the understanding of these processes. Recently, Zheng *et al.*[13] modified a sampling method, denoted army ants tunneling,[14] to overcome the accuracy deficiency for ground state reactions simulations using precomputed PES associated with (semi-)classical trajectories or for methods with the wave packets following a classical trajectory. The method uses a sampling different from the uniform sampling method which would sample rare events too seldom for any accuracy. The army ants tunneling approach uses one weighting scheme for the selection of path to follow—with a bias to

explore and sample rare events often—and another to compute the resulting reaction rates and other properties. The recent modification to this scheme[13] involved the use of internal coordinates describing the tunneling path. In a subsequent publication[15] they generalized the approach to non-adiabatic simulations, which makes it relevant to photochemical investigations. The scheme shows much improved convergence of the non-reactive probability with respect to the length of the trajectory simulations.

In the adiabatic description, the non-adiabatic coupling vectors represent the coupling between adiabatic states. These coupling vectors are erratic close to—and singular at—CIXs, making them difficult to use in dynamics simulations based on precomputed PES and coupling vectors represented in the adiabatic representation. This problem is reduced or eliminated by diabatization methods—complete or partial—in which the adiabatic states are rotated to find new representations in which the coupling is negligible or significantly reduced. The diabatization, however, has a major flaw, it is not uniquely defined. Moreover, the diabatic states and their associated PES depend on the number of states considered. Hence, there is a need to define such methods in a pragmatic way, which produces sufficient decoupling and robustness with respect to the number of states considered, while still not being computationally demanding. Some such methods are purely numerical, while others are based on some chemical intuition, or a combination of both. One such method is the so-called fourfold way.[16] This approach is based first on the construction of diabatic molecular orbitals (DMOs) using a three-fold density criterion and second a sometimes enforced fourth criterion based in reference orbitals. This is then followed by the so-called configurational uniformity step in which the diabatic states are to have optimal overlap with reference configuration state functions (CSFs).[17] The past implementation of this approach was based on multi-configurational self-consistent field (MCSCF) or quasi-degenerate perturbation theory (QDPT). The option of doing this on the correlated level of theory is important. Dynamic electron correlation can have significant impact on the relative position of the PES of the adiabatic states (see Fig. 4 for an example for LiF with wavefunction models which do not and do include dynamic electron correlation). This significant change of the relative position of PES and the location of the avoided-crossing region will have a significant impact on the quality of the diabatic states and their effectiveness in reducing or eliminating the non-adiabatic coupling between the states. In the original implementation,[16] the MCSCF results using the adiabatic or the diabatic MOs give identical energetics. This was not the case when the four-fold way was applied to QDPT generated DMOs. This discrepancy was solved *ad hoc* by defining the adiabatic energies as those computed with the DMOs rather than the canonical orbitals. Subsequent checks of the validity of this approximation displayed insignificant energy differences for a small set of test molecules. However, for a recent application to the thioanisole molecules a discrepancy of 0.8 eV was found. It initiated the development of an improvement—the model space diabatization (MSD) scheme.[18] The new

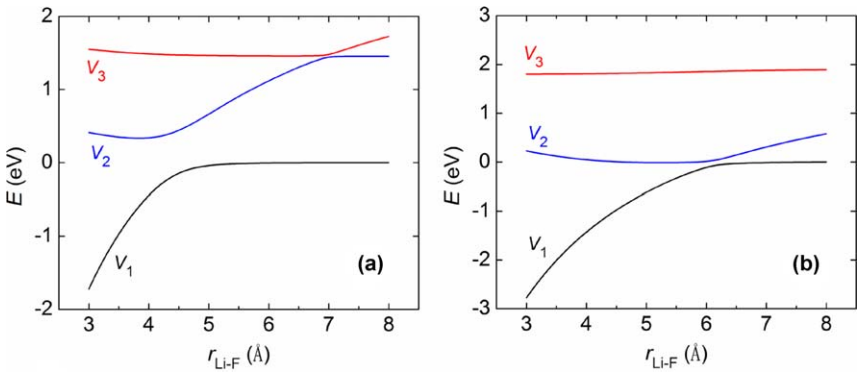

Fig. 4 Adiabatic potential energy curves of LiF as functions of the internuclear distance for (a) the SA-CASSCF (no dynamic correlation) and (b) the extended multiconfiguration (XMC)-QDPT methods. [Reprinted from *J. Chem. Phys.*, 2015, **142**, 064106, with permission of AIP Publishing LLC.]

method uses information from the four-fold way diabatization performed at the state-average (SA)-CASSCF level of theory and QDPT results to generate the final diabatization. The MSD procedure is a rather trivial procedure which involves some additional unitary transformation steps. In the MSD formalism, the diagonalization of diabatic potential energy matrix exactly reproduces the adiabatic states and associated energies.

It has for a long time been a dream to control and manipulate the dynamics of the nuclear wavepackets for excited states by modulating the light which interacts with the molecular system. This would lead to new possibilities to explore and utilize reactions paths not accessible under conditions of standard laser pulses—the so-called polarized Π pulses. In particular, closed loop-learning algorithms have been used to optimize spatial and temporal shape of the external electromagnetic field. While this is a successful approach, it often achieves results without any understanding of the underlying molecular mechanism. Alternative methods have been offered as the so-called optimal control theory approach which, however, requires multiple solutions to the time-dependent Schrödinger equation. This renders the approach only applicable to rather small systems. Recently, Tavernelli and co-workers[19] proposed an alternative—the so-called LCT approach. This approach allows for the derivation of the shape and time-evolution of the interacting electromagnetic field on the fly in a TSH simulation. The same authors demonstrated the usefulness of this in association with the simulation of the excited-state proton transfer of 4-hydroxyacridine (4-HA) at the DFT level of approximation.[20] The LCT approach is based on that the electromagnetic field is modified on the fly in a linear fashion to increase the value of a specific property with respect to time. In the recent report,[20] the target is to optimize the population of the S_1 state of 4-hydroxyacridine, in which a proton transfer takes place. The authors do this for 6 different TSH trajectories and the Fourier transform of the individual pulses exhibits significant similarities, thus making it

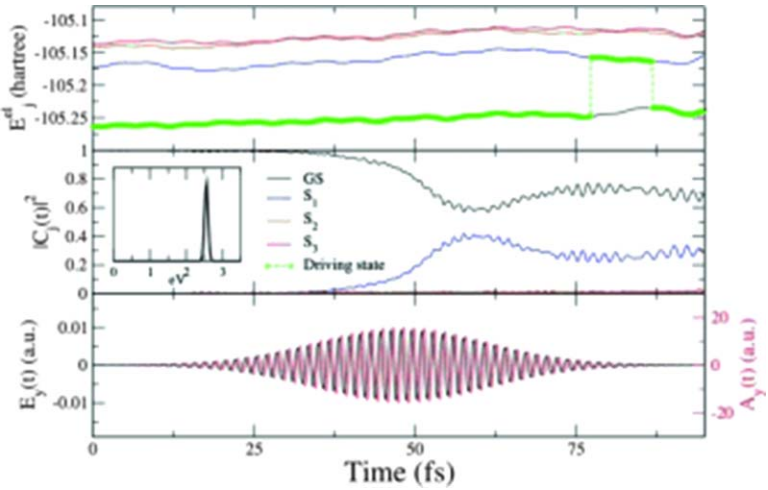

Fig. 5 Dynamics of 4-HA under the action of a polarized Π pulse with central frequency $\omega = 2.55$ eV. Top panel: Time series of the potential energy curves obtained with DFT calculations. Color code: GS (black), S_1 (blue), S_2 (orange) and S_3 (red). The green line with circles highlights the force (driving) state. Middle panel: Probability of each state for one trajectory. The inset shows the Fourier transform of the entire Π pulse. Bottom panel: Applied vector potential component (—) and corresponding electric field (—). [Reprinted from *ChemPhysChem*, 2015, **16**, 2127, with permission of John Wiley and Sons. © 2015 WILEY-VCH Verlag GmbH & Co. KGaA, Weinheim.]

plausible that an ensemble averaged pulse would optimize the desired property. It is clear from the simulations that a polarized Π pulse targeting the excitation energy at the Franck–Condon region will only be partially successful in populating the S_1 state (see Fig. 5). Here the final occupation of the excited state ends up at about 40%. This in stark contrast to the picture of the LCT driven simulation (see Fig. 6) in which the population of the S_1 state at the end of the pulse is almost 100%. Further studies are needed and in particular the effectiveness of an ensemble-derived average pulse to optimize a target condition needs to be established.

The symmetrical windowing technique was recently proposed as a microscopical time-reversal approach towards computing reaction probabilities in quasi-classical approaches (SQC).[21] In particular, the study showed that using Gaussian type windowing functions with a 1/2 width unit reproduces quantum mechanical results for the reaction probabilities of the vibrational states in the collinear $H + H_2$ reactive scattering process. In a recent extension of the method Miller and co-workers[22] have extended the approach to non-adiabatic processes over multiple electronic states. In the study of a model photoinduced proton-coupled electron transfer process, they demonstrated that the SQC approach gives a reasonable population decay as compared to Marcus theory. The authors noted that ''non-adiabatic effects may be incorporated into detailed simulations of complicated molecular processes by simply introducing an auxiliary pair of 'electronic' action-angular variables.'' Subsequent semi-classical simulations treat these variables on the same footing as the other classical variables.

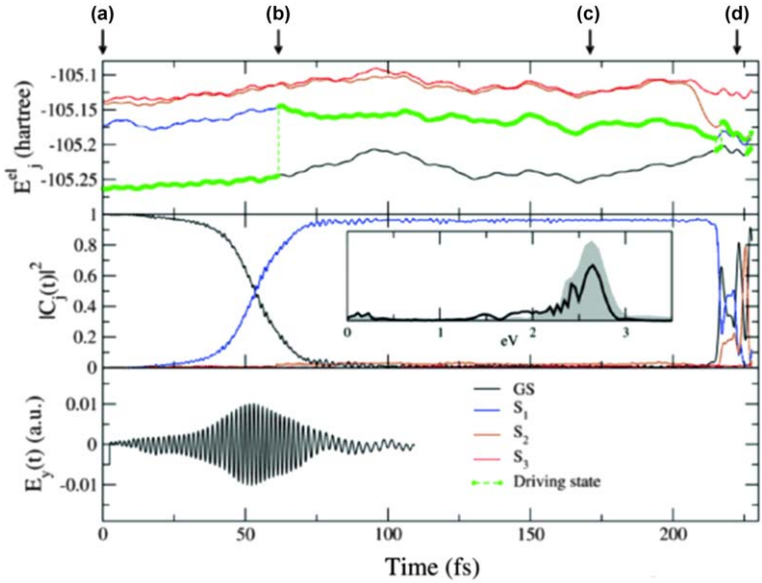

Fig. 6 TSH/LCT dynamics of 4-HA, representative trajectory 1. Top panel: Potential energy curves obtained by using DFT/PBE and LR-TDDFT/PBE/TDA calculations. Color code: GS (black), S_1 (blue), S_2 (orange) and S_3 (red). The green line highlights the force (driving) state. Middle panel: Occupations (equation image) of all relevant electronic states along the same trajectory. The inset shows the Fourier transforms computed for the entire LCT pulse (—) and for the first part of the pulse until the trajectory hop occurs (light gray area). Bottom panel: Computed local control pulse. [Reprinted from *ChemPhysChem*, 2015, **16**, 2127, with permission of John Wiley and Sons. © 2015 WILEY-VCH Verlag GmbH & Co. KGaA, Weinheim.]

Finally, some brief comments on the work by Nance and Kelley on the use of a reformulated Smolyak's sparse grid interpolation algorithm in association with molecular dynamics simulations.[23] This algorithm is used in the context when diabatic PESs have been determined and are expressed by analytic functions in subsequent trajectory simulations. The use of the new algorithm is substantially more efficient and faster (by 5–8 times) as compared to standard techniques. This both with respect to (a) increased accuracy of the interpolated surfaces, for the same number of grid points, as compared to the exact ones, and (b) to the increased dimensionality of the interpolated surfaces.

2.3 Reviews

During 2014–2015 a number of extensive and rich review papers related to molecular dynamics were published. We will simply mention the reviews here and invite the interested reader to consult the papers for details—it would be grossly redundant for us to comment any further on these manuscripts here in this brief presentation. Morokuma and co-workers[24] published an extensive review of the usefulness of the so-called global reaction route mapping (GRRM) approach as an instrument for the unbiased investigation of possible photo chemical reaction paths of a molecular system. González and co-authors[25] presented a review of the

state of the art with respect to TSH simulations in association with intersystem crossings (ISC), *i.e.*, spin-forbidden processes. Furthermore, excitation transport in photosynthetic complexes approximated at the quantum mechanical level was reviewed by Levi *et al.*[26] Hynes and collaborators[27] published a perspective on non-adiabatic dynamics in association with TSH. The same topic but with the aspect of a comparison between direct approaches *vs.* the full QMD approach were reviewed by Persico and Granucci.[28] Wormit *et al.*[29] published an overview of the use of the algebraic diagrammatic construction (ADC) method for excited states. Finally, Blancafort[30] presented an excellent review on photodynamics at the seams of CIXs; the review contains a number of illustrative examples. Again, the interested reader is recommended to read these detailed reviews for further information.

3 Mechanisms of DNA/RNA damage and repair

Life on Earth as we know it is the result of a delicate equilibrium between stability and reactivity of nucleic acids. Maintaining the structural integrity of DNA/RNA macromolecules is crucial for living beings. These biopolymers compose the genotype, which contains all the instructions needed to control the cellular machinery ready to be executed at the precise moment. On the other hand, life needs to adapt to changeable environments and therefore requires some flexibility in the genetic information in order to adjust these instructions to new conditions. Thus, completely immutable DNA/RNA molecules are also not compatible with life. In this framework is where we can define the subtle equilibrium between DNA/RNA integrity and damage arises.

As mentioned in the Introduction, in order to make a tribute to the International Year of Light and Light-Based Technologies and the Nobel Prize awarded to the field of research on DNA, some recent advances in theoretical photochemistry on DNA/RNA photostability and damage will be highlighted in the present section. The photoprocesses are classed according to the type of interaction with the DNA nucleobases (NBs). Thus, the direct effect of UV-light in the canonical NBs will be considered first. Second, we will review recent findings on the photophysics and photochemistry of modified NBs. Third, we will present new contributions on the understanding of DNA photosensitization. Next, studies on DNA damage mediated by ROS and low-energy electrons (LEE) will be provided. Finally, the section will end with recent contributions on DNA interactions with other species such as aminoacids and metals.

3.1 Direct UV-light interaction with canonical DNA/RNA nucleobases

UV light coming from the Sun interacts with DNA/RNA and has the ability to induce mutations in the NB sequence, which allows the evolution of species but also the development of serious diseases like skin cancer.[31] Light is mainly absorbed by NBs populating singlet excited states with an excess of energy that, in a majority of cases, is dissipated in a non-reactive and non-radiative manner through accessible S_0/S_1 CIXs.[32,33] Even

though the underlying molecular mechanisms are in general well understood,[34] some aspects are still not clear. In this context, remarkable contributions were published in the years 2014 and 2015. One aspect involves the absorption process of light, which is in general assumed to take part in a single NB.[32]

However, shifts may arise in larger multi-chromophoric systems when additional adjacent NBs are considered.[34] Blancafort *et al.*[35] recently reported electronic coupling between the bright $\pi\pi^*$ excited states in NB dimers of 0.05–0.14 eV, which were obtained with the multistate (MS)-CASPT2 method. Moreover, Ramazanov *et al.*[36] studied a collection of DNA dimers, computing red shifts up to 0.6 eV with respect to the B-DNA orientation. The authors concluded that highly distorted arrangements of the dimers could absorb in the $\sim$300 nm region, where the single monomers are mostly transparent.

The radiationless decay mechanism of the DNA/RNA nucleobases still remains a hot topic in computational photochemistry. Barbatti[37] reported a new de-excitation mechanism for the 7*H*-adenine tautomer based on ADC(2) nonadiabatic dynamics simulations. The non-adiabatic process takes place *via* an initial step of electron transfer from a surrounding water molecule. For 9*H*-adenine, the ultrafast mechanism was revisited by Tuna *et al.*[38] taking into account also the corresponding 2-deoxyribose moiety in the computations. The obtained results at the ADC level showed that an excited-state intramolecular proton transfer between the NB and the sugar opens a new decay route *via* a more accessible S_0/S_1 CIX than that of the intrinsic one localized in adenine. Furthermore, in the nucleoside, there are other possible photoreactions between the NB and sugar moieties which could be relevant in the selection of the building blocks of life during the prebiotic era. Regarding these possibilities, Szabla *et al.*[39] studied by means of the CASPT2//CASSCF methodology the photoanomerization process observed experimentally in 2′-deoxycytidine after light irradiation. The mechanism proposed by the authors is an excited-state hydrogen atom abstraction at the sugar C1′–H position by an oxygen atom of cytosine (see Fig. 7), followed by a subsequent release of the hydrogen atom in the ground state with a small barrier of 10.8 kJ mol^{-1}. In two other studies, the ultrafast decay mechanism of isolated uracil[40] and cytosine[41] was used to test a new theoretical method for simulating femtosecond stimulated Raman spectroscopy signals and to carry out a benchmark of DFT functionals, respectively.

The excited-state interaction of two stacked NBs was also studied in the 2014–2015 period. Conti *et al.*[42] explored the photochemical channels of two stacked adenine molecules using a combined quantum mechanics/molecular mechanics (QM/MM) computational approach. The CASPT2 results support the decay through a localized L_a state, discarding the participation of a charge-transfer state. Regarding two stacked pyrimidine NBs, they can lead to the formation of excimers, defined as minima in the excited state surface, which evolve under certain conditions to the production of cyclobutane pyrimidine dimers (CPDs). These photoproducts are considered as one of the most common flaws

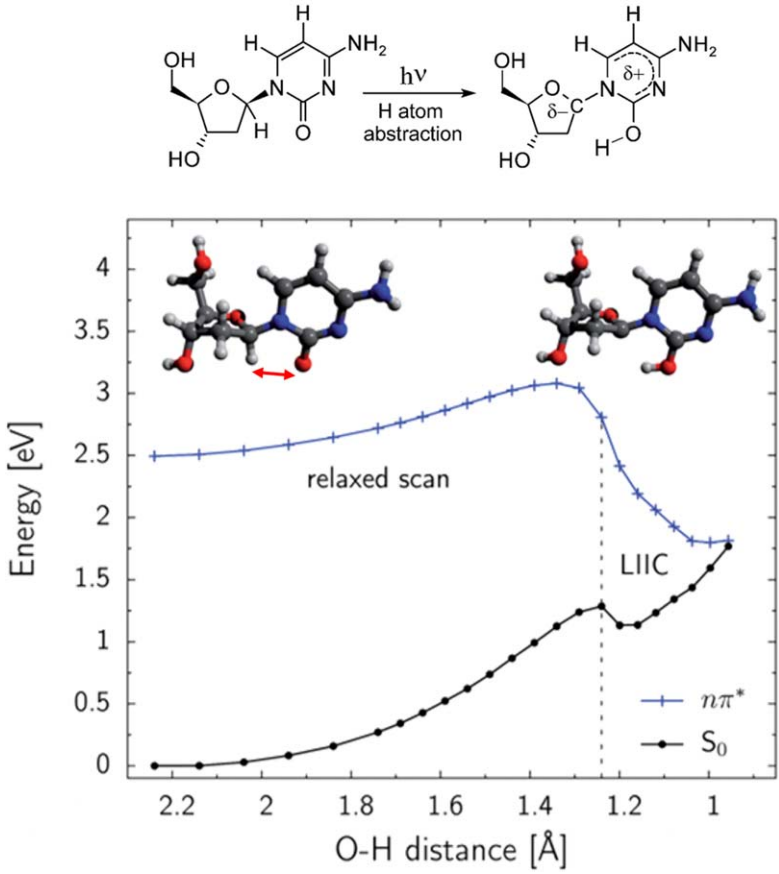

Fig. 7 Potential energy surfaces of the $n\pi^*$ and the ground state along the O–H hydrogen-transfer coordinate. [Adapted from *Chem. Sci.*, 2015, **6**, 2035 with permision from the Royal Society of Chemistry.]

observed in DNA/RNA structures after exposure to UV radiation, and therefore this type of photoreactions was also studied by the computational photochemists. Barbatti[43] explored with the DFT and second-order approximate coupled-cluster (CC2) methods the dimerization and repair mechanisms of the thymine dimer on the singlet, triplet, doublet anion, and doublet cation manifolds. The author found a new minimum on the S_0 surface with a methylmethylidene-hexahydropyrimidine structure (see Fig. 8). The cytosine dimers were also studied by Yuan *et al.*[44] who performed semiclassical dynamics.

Since CPDs represent serious lesions that can induce mutations in DNA sequences, cells are obliged to repair the damage in order to retrieve the original DNA structure. In 2014, the CPD repair mechanism by the photoliase enzyme was studied by Wang *et al.*,[45] who used the CASPT2//CASSCF/AMBER approach. The authors proposed a proton-coupled electron transfer taking place in the S_2 state as the initial step in the reparation mechanism.

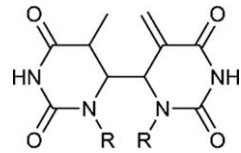

Fig. 8 Structure of themethylmethylidene-hexahydropyrimidine minimum in the S_0 surface of the thymine dimer.

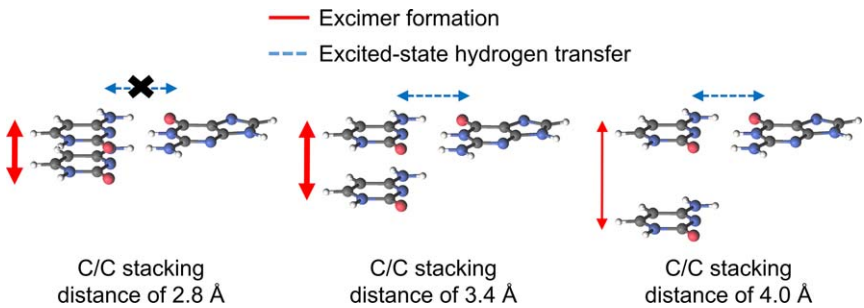

Fig. 9 Schematic representation of the competition between the intra-strand excimer formation and the inter-strand double hydrogen transfer in the GCC trimer, at C/C stacking distances of 2.8, 3.4 and 4.0 Å.

Studies on more complex photochemical events occurring in DNA/RNA trimers have also been recently reported. The competition between the excimer formation and the excited-state hydrogen transfer processes in a guanine–cytosine/cytosine trimer model was assessed by Francés-Monerris *et al.*[46] using the multiconfigurational CASPT2//CASSCF strategy. The effect of the face-to-face π-stacking distance between the cytosine molecules on the intra-strand formation of excimers and the inter-strand double hydrogen transfer was evaluated mapping the relevant electronic states along the appropriate N–H coordinates. The obtained results indicate that only at short stacking distances (2.8 Å) the hydrogen transfer is significantly hindered, whereas at the rest of arrangements the transfer is operative (see Fig. 9). Additionally, the authors found that at the tautomerization region the excimer formation is less favorable that at the Watson–Crick area. This fact might prevent the accumulation of lesions in DNA. The tautomer formation through the excited-state hydrogen transfer mechanism studied in the theoretical work[46] has been recently measured, with a yield of 10%.[47] Regarding tetrameric models of DNA, the impact exerted by adjacent NBs to the thymine–thymine CPD formation was evaluated by Lee *et al.*[48] using a combination of the umbrella sampling and the QM/MM approaches and considering a set of three ATTA, CTTA, and GTTA tetramers. A new decay pathway was found, involving a charge-transfer state between the flanking NBs which leads to the formation of an excimer followed by a non-reactive decay. The authors concluded that the flanking NBs quench the excited states of the thymine–thymine dimer and therefore prevent the formation of harmful CPDs.

Remarkable advances in the theoretical simulation of bidimensional (2D) electronic spectra were made in the years 2014 and 2015 by the group of Garavelli and coworkers.[49,50] The 2D spectroscopy allows the disentanglement and subsequent tracking of mixture of excited states present in multichromophoric systems. The results reported for adenine monomer[51] and dimer[52] showed that it is possible to decouple the localized states traditionally detected as a unique signal with conventional techniques.

3.2 Photophysics and photochemistry of modified DNA/RNA nucleobases

The study of modified NBs remains as a very active research topic in modern photochemistry,[53] not only because natural modifications are constantly produced in DNA, but also because unrevealing the photophysical and photochemical properties of these compounds boosts the understanding of the intrinsic properties of canonical NBs. Lu *et al.*[54] determined with the MRCI method the excited-state relaxation of 8-oxoguanine (see Fig. 10), which is one of the most abundant products encountered in conditions of oxidative stress. Neutral 8-oxoguanine exhibits a unique ultrafast decay to the ground-state, whereas the deprotonated system has two decay channels with significant energy barriers. The theoretical results allowed the interpretation of the spectroscopic data reported in the same work. Moreover, the excited-state relaxation of both neutral and anionic systems were studied by Tuna *et al.*[55] in the 8-oxo-deoxyguanosine. The authors found an intramolecular excited-state proton transfer between the N_3 position of guanine and the 5′-OH hydrogen of the sugar, which is accessible in the neutral form, but hampered in the anion system. Therefore, these results also support the more intense fluorescence observed for the latter system.

Modified NBs also play a central role in the design of potential photosensitizers (PSs) for photodynamic therapy.[56] This technique is used in the

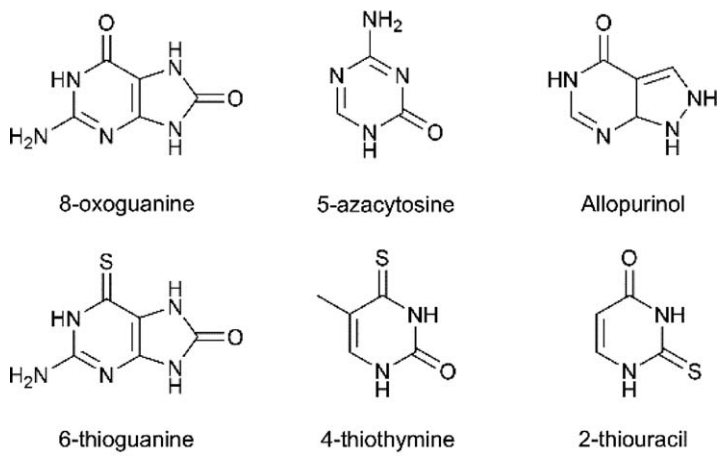

Fig. 10 Structures of the modified NBs reviewed in the present chapter.

treatment of many tumors and other diseases like viral infections.[57] In general, the destruction mechanisms require the population of long-lived triplet states of the PSs, able to trigger energy transfer processes either directly to DNA (type I process) or to triplet oxygen (type II process) producing singlet oxygen.[58] For this reason, a usual goal in this area of research is to find candidates with large spin–orbit couplings (SOCs) and relatively stable triplet states able to transfer the energy *via* triplet–triplet energy transfer to the surroundings. Since heavier atoms provide, in general, larger SOCs, O→S replacements in DNA/RNA nucleobases have been used in cancer treatment.[59,60] In this context, Martínez-Fernández *et al.*[61] focused their attention on 6-thioguanine (see Fig. 10) and determined the evolution of the molecule on the excited-state PESs employing a direct surface hopping dynamics approach. The results revealed in this case that the contribution of the triplet was significant. Thus, the main relaxation path leads to the population of the T_1 state, which exhibits a relatively long lifetime. Thereby, the postulated mechanism is able to explain the photosensitivity of patients prescribed with this drug.

Other thio-modified NBs were studied by Cui *et al.*[62] and Gobbo and Borin,[63] which described a similar behavior for 4-thiothymidine and 2-thiouracil, respectively. In these systems, the preferred excited-state decay also leads to the population of the lowest-lying T_1 state. C→N modifications were also studied, motivated by their role as chemotherapeutic agents.[55] In 2014, Giussani *et al.*[64] documented the decay mechanism of 5-azacytosine (see Fig. 10), predicting a dark $n_N\pi^*$ state below the bright $\pi\pi^*$ state. The computational results indicate that the ultrafast relaxation takes place through two accessible $S_2(\pi\pi^*)/S_1(n_N\pi^*)$ and $S_1(n_N\pi^*)/S_0$ CIXs, instead of the direct $S_1(\pi\pi^*)/S_0$ CIX found in natural NBs. The findings also showed a minor contribution of the triplet state in the photophysics of this modified NB. Ultrafast decay to the ground state was also predicted for allopurinol, a purine NB analogue.[65] Here, CASSCF/MM dynamics calculations revealed that the solvent (water) significantly increases the S_1 lifetime compared to the results *in vacuo*.

3.3 DNA photosensitization mechanisms

DNA damage by triplet states can also be achieved by exogenous species which are not necessary integrated in the DNA structure.[66] Here, computational photochemistry is a powerful tool used to unravel the molecular mechanisms behind the photosensitization processes[67] and therefore to design compounds that fulfil the required conditions. The photosensitization ability of arylketones, in particular acetophenone and benzophenone (see structures in Fig. 11), was studied in 2014–2015 by Huix-Rotllant *et al.*[68] and Sergentu *et al.*,[69] respectively. In the former, an ultrafast population of the T_1 lowest-energy triplet state of acetophenone was suggested as a plausible process at the Franck-Condon vicinity *via* a quasi-degenerated area between the singlet and triplet manifolds. For benzophenone,[69] the proposed mechanism consists of a two-step process in which an intermediate state (T_2) is primarily populated in the

Franck-Condon region. Then, the system evolves in this state directly to a CIX with the lowest-energy triplet state (T_1). It is known that the triplet state lives enough to photosensitize other systems with triplet states in the same range of energies. More recent studies, carried out by Dumont *et al.*,[70] focused on the photosensitization mechanism of benzophenone to thymine in the DNA. In this case, the authors used the QM/MM strategy and the TDDFT and CASPT2 methods to model the triplet–triplet energy transfer process from benzophenone to the NB. Small barriers (<0.1 eV) were determined when benzophenone is intercalated in the DNA strand. Additionally, a significant stabilization of the low-lying triplet state of thymine with respect to previous gas-phase calculations was also found in the study.

Another relevant family of effective PSs are the phenotiazinium dyes. For methylene blue (MB, see structure in Fig. 11), Nogueira *et al.*[71] reported significant differences between the inter-system crossing mechanisms in water and in DNA (see Fig. 12). The theoretical results indicate that, in solution, hydrogen bonding between the PS and water molecules from the surroundings quench the electronic SOC. On the contrary, in DNA, solvation is less effective and therefore both electronic

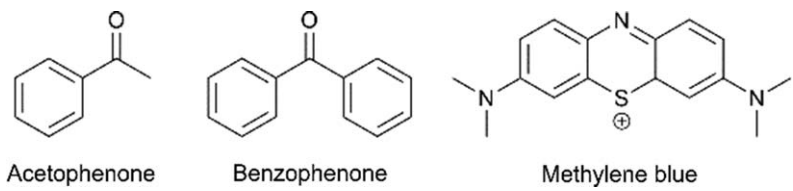

Fig. 11 Structures of the PSs reviewed in the present chapter.

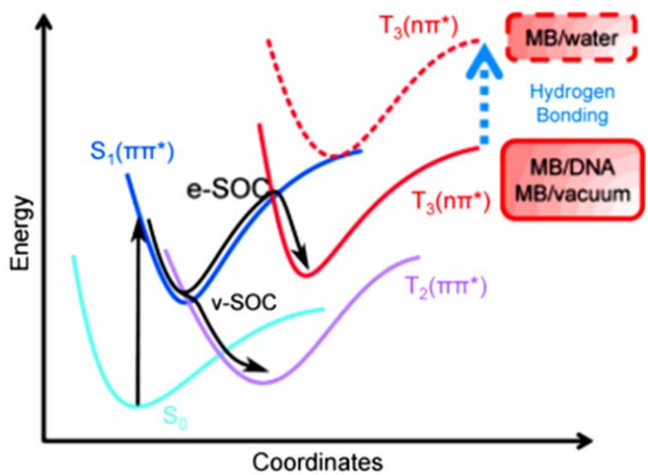

Fig. 12 Schematic comparison between the population of the triplet states of methylene blue (MB) both in water and at DNA environment. Water solvation destabilizes the $T_3(n\pi^*)$ state. [Reprinted from *Angew. Chem., Int. Ed.*, 2015, **54**, 4375, with permission of John Wiley and Sons. © 2015 WILEY-VCH Verlag GmbH & Co. KGaA, Weinheim.]

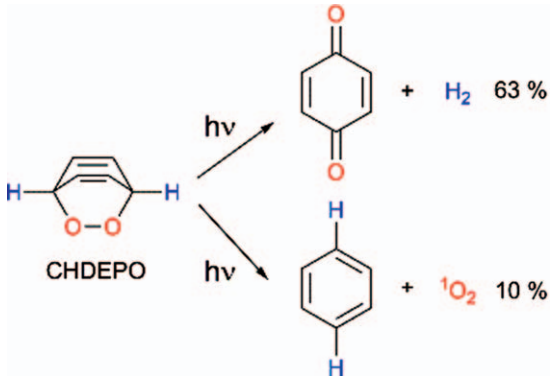

Fig. 13 Photochemical decomposition of CHDEPO.

and vibronic SOC mediate the ISC processes, increasing thus the efficiency of the photosensitization process.

DNA photosensitization using transition metals complexes was also an intense field of research in the years 2014 and 2015. Ru(II)-compounds were suggested to induce light-mediated damages to DNA[72–75] and Zn(II)-complexes were investigated as potential singlet oxygen generators.[76,77] Alternative procedures of singlet oxygen production were also proposed using metal-free compounds. For example, Martínez-Fernández *et al.*[78] described the photo-release of singlet oxygen from cyclohexadieneendoperoxide (CHDEPO) (see Fig. 13). The results from *ab initio* surface hopping dynamics point to the O–O homolysis as the most favorable photochemical channel (63%) and the singlet oxygen production quantum yield was computed to be of 10%.

3.3.1 DNA damage by reactive oxygen species. ROS constitute a family of compounds capable to react with DNA and to alter the structure of NBs, which can lead to mutations and/or strand breaks.[67] One of the most reactive ROS is the OH radical, which undergo fast reactions with NBs and sugars. It has been established that $^{\bullet}$OH adds preferentially to the C5=C6 bond of pyrimidines, forming transient C-centered radicals that live in the μs scale. To detect such reactive species, transient absorption spectroscopy can be used together with computational photochemistry. The latter allow an accurate assignment of the spectra.

In 2014, Francés-Monerris *et al.*[79] studied the C5 and C6 adducts of uracil (see Fig. 14) by means of the multiconfigurational CASPT2//CASSCF approach.[80] In contrast to the C5 product, the C6 adduct is able to absorb light in the visible range (~406 nm) populating the corresponding D_3 state, which implies a redistribution of the unpaired electron among the π orbitals.

The authors also explored the photochemistry of the C6 adduct. An excited state characterized by the localization of the spin density at the lone pair orbital of the OH oxygen (n_{OH}) was also found at accessible energies. The characterization of the PESs of the ground and lowest-lying excited states along the C6–OH stretching coordinate revealed an available photochemical route which involves the photo-release of the $^{\bullet}$OH

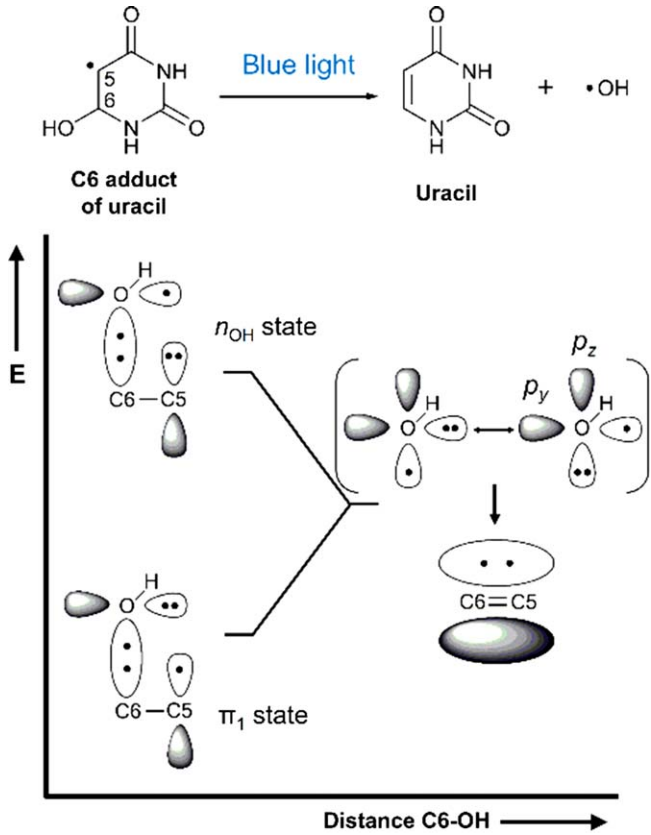

Fig. 14 Schematic representation of the possible photo-dissociation process of the OH adduct of uracil at C6 position. Left hand side corresponds to the Franck-Condon region of the adduct, whereas the right hand side represents uracil + •OH at an infinite distance. [Adapted with permission from *J. Phys. Chem. B*, 2014, **118**, 2932. Copyright 2014 American Chemical Society.]

species. This constitutes a possible repair channel after oxidative damage (see Fig. 14). However, further theoretical and experimental studies are required to determine the quantum yield of this route.

3.3.2 DNA damage by low-energy electrons. Secondary LEEs are formed in biological media exposed to ionizing radiation and also as a consequence of metabolic processes.[81] These interact with DNA/RNA nucleobases yielding two types of anions in the gas phase: (a) dipole-bound (DB), where the extra electron is located in the positive part of the dipole of the NB, and (b) valence-bound (VB), where the electron occupies a π^* orbital.[82] Since LEEs can produce single and double strand breaks,[83] many scientist have spent efforts to understand how NBs and LEE interact. Gas-phase experiments with isolated NBs were early carried out as a first step towards the comprehension of such DNA damage. It was shown that the NBs looses hydrogen atoms from the N–H bonds.[84]

Since then, most of the studies have focused on the ground-state reactivity and much less information can be found in the literature about

the excited states. One of the computational studies taking into account the excited state was carried out in 2015 by Francés-Monerris *et al.*,[85] who provided new insights into the unimolecular decompositions of all the five DNA/RNA NBs by using the CASPT2//CASSCF methodology. The results suggest that both DB and VB anions should be involved in the gas-phase fragmentations. Moreover, the first and second vertical electron affinities of the pyrimidine NBs indicate that the π_1^- state is responsible of the H-loss at $\sim$1 eV, whilst the π_2^- state participates at energies close to $\sim$2 eV. Minimum energy path (MEP) calculations on the π_2^- excited states allowed to establish the corresponding thresholds for the π_2^- participation in the fragmentation processes. On the basis of the reported theoretical data, the authors were able to assign the experimental signals.[84]

3.3.3 DNA interaction with other species. Interaction between DNA nucleobases and other species different from those mentioned in the previous sections was also the target of computational studies in 2014–2015. Amino acids and metals are common examples. Thus, the photoinduced cross-link between NBs and aminoacids was studied in the 5-benzyluracil model by Micciarelli *et al.*[86] The authors proposed a mechanism for its photo-cyclization after irradiation with UV light, which was based on both spectroscopic and theoretical (TDDFT) data. On the other hand, the influence exerted by a complexed metal (Ag^+) on the electronic properties of cytosine was reported by Taccone *et al.*[87] The authors showed that the metal induces a charge-transfer phenomenon from a π orbital of the NB to the Ag^+ counterpart, yielding as a result the corresponding cytosine cation and the neutral metal.

4 Photo-induced mechanisms of relevance in biology and technology

Several computational studies were carried out with relevant applications in biology and technology in 2014 and 2015. We shall mainly focus here on those works performed with accurate multi-reference methodologies which we consider are the most appropriate for a balanced characterization of the distinct nature of excited states involved in photochemical phenomena. Single-reference methods have been improved in the last decade, allowing the treatment of large-size molecular systems with accuracy in well-calibrated electronic-structure problems. Nevertheless, they do not have the general applicability of multi-reference methods as yet. We exclude DNA studies here, since they where reviewed in the previous section.

As in previous volumes,[3–5] we found in the reviewed period works that can be classed according to the type of photoinduced process studied as *E*/*Z* photoisomerizations involving C=C and N=N double bonds, excited-state hydrogen/proton transfer processes, photodissociations/photocycloadditions and ring-opening/ring-closure mechanisms. Photophysical processes that involve the production of two emissive states, charge separation and singlet fission were also topics of intense research.

In the following we will briefly summarize the main trends that we have observed in the published articles.

4.1 *E*/*Z* photoisomerizations

This type of excited-state chemistry is very important in biology since it represents the production of molecular motion as a response to the stimulus of light. The computational studies performed in the last two years focused mainly on the isomerization mechanisms related to the process of vision in vertebrate and invertebrate organisms (retinal) and those present in certain bacteria to trigger photo-mobility and biological responses (photoactive yellow protein, PYP). In the first case, most of the efforts of research were spent into the study of photochemical process in the bovine rhodopsin, which corresponds to the 11-*cis* to all-*trans* isomerization of the retinal protonated Schiff base.[88] Walczak and Andruniow[89] analyzed by using the CASPT2//CASSCF/MM hybrid approach the effects of retinal polyene (de)methylation on the photo-isomerization mechanism. Garavelli and co-workers[90,91] showed the advantages of transient 2D electronic spectroscopy to track the evolution of the excited states of retinal along the photoisomerization path. The 2D spectroscopy was also used to study the excited-state dynamics of carbonyl carotenoids.[92] Martínez and co-workers[93] carried out full multiple spawning dynamics with a hybrid QM/MM method to compare the excited-state isomerization lifetimes of the retinal protonated Schiff bases *in vacuo*, neat methanol solution, and methanol solution with a Cl counterion. Olivucci and co-workers[94,95] performed a couple of works in which the isomerization mechanisms of distinct types of retinal-based enzymes were compared by using multiconfigurational QM/MM methodologies. In particular, the photo-induced isomerization of the bovine rhodopsin was first compared with the sensory rhodopsin from the cyanobacterium *Anabaena* PCC 7120 and second with other squid visual photoreceptors and the human nonvisual photoreceptor melanopsin. Other types of rhodopsins studied were the channel rhodopsins, which function as light-gated ion channels,[96] and the isorhodopsin, which involves the isomerization of 9-*cis* retinal instead of that of 11-*cis*.[97]

Regarding the PYP chromophore, Wei *et al.*[98] performed a CASPT2//CASSCF/AMBER QM/MM study of the overall photocycle process. The (a) hula twist, (b) bicycle pedal, and (c) one-bond flip mechanisms of isomerization were compared. These distinct types of mechanisms might take place in chains of conjugated double bonds. They correspond to (a) configurational isomerization at one double bond and conformational isomerization at an adjacent single bond, (b) isomerization at two formal double bonds, and (c) torsional relaxation around one formal double bond. Martín and co-workers[99] carried out two computational studies on models of the PYP, by using the averaged solvent electrostatic potential from molecular dynamics (ASEP/MD) approach, to analyze how solvent and also the substitution of sulfur by oxygen atoms and hydrogen by methyl in the coumaryl tail affects the UV-Vis absorption spectrum.

The *E*/*Z* photo-induced isomerization is also of interest in technology for the same reasons as above – the possibility of producing molecular motion as response to light. Here, biology has inspired the design of photoswitches with efficient transformations of light energy into molecular motion.[100] In this context, we have found non-adiabatic dynamics studies with *N*-akylated indanylidenepyrroline Shiff bases.[101,102] Two aspects to take into account in order to search for more efficient molecular rotors are the directionality of the rotation and the shape of the CIX involved in the isomerization process.[103,104] Green fluorescence protein analogues, in particular arylidenehydantoins, also showed promising applications as molecular photoswitches.[105] Furthermore, the PYP chromophore was proposed for electrochromic applications, such as optical memories. As described by Groenhof, Boggio-Pasqua and co-workers,[106] the direction and strength of external electric fields are able to control the bond selectivity for isomerization and its efficiency. Other common molecules in this field are aromatic azo compounds.[107,108] In this case, Gámez *et al.*[108] reported an enhancement of the isomerization process in 2-aminoazobenzene due to an intramolecular hydrogen bond which weakens the N–N bond. Meanwhile, Frutos and co-workers[109] chose azobenzene to show how photoswitches might be controlled by external mechanical forces.

The sunscreen industry also benefits from the *E*/*Z* isomerization process induced by UV light. Chang *et al.*[110] studied the photo-protection mechanism of *p*-methoxymethylcinnamate by using the CASPT2 method. In this study, the authors show how water molecules are able to enhance the efficiency of the protection mechanism. The mechanism of photoprotection of another molecule, gadusol, was studied by Sampedro and co-workers.[111] In this case, the relaxation channel implies an evolution towards an ethylene-like CIX which allow the transfer of population back to the ground state. However, since the double bond is part of a cycle, isomerization cannot take place and the original configuration of the atoms is recovered.

Finally, in order to show the basic electronic-structure and mechanistic properties of a *E*/*Z* photoisomerization, we will describe in more detail a study carried out by one of the authors in the present review in 2015 in collaboration with the experimentalists El-Zohry and Zietz.[112] The molecule studied was indoline, which is the donor moiety in different dyes used in dye-sensitized solar cells. In these photovoltaic devices, in order to allow a highly efficient electron injection to the conduction band of TiO_2 at the electrode, competitive decay channels must be avoided. However, very fast decay signals (20–40 ps) are measured experimentally in the indoline-based dyes. To interpret these signals, we used the CASSCF/CASPT2 method and characterized the PESs of the ground and lowest-lying excited state along the torsion and pyramidalization coordinates related to the exocyclic double bond. As displayed in Fig. 15, these nuclear distortions brings the excited molecule towards a region of crossing between the two lowest-lying states, which allows the energy deactivation and recovery of the original

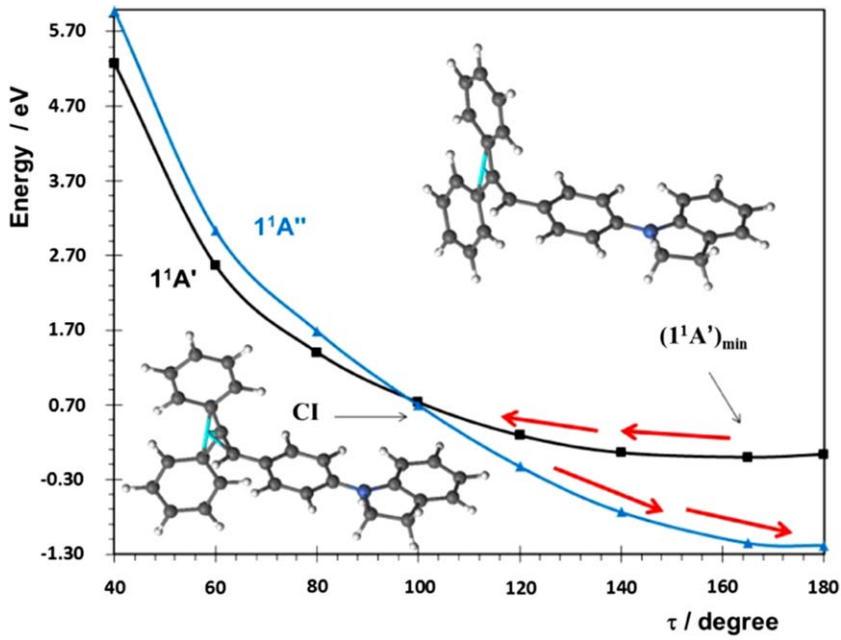

Fig. 15 CASPT2 energies of the ionic ($1^1A'$) and biradical ($1^1A''$) states at different pyramidalization angles. The structures for the CIX and excited-state minimum $(1^1A')_{min}$ are shown. The ghost atom (in cyan) helps to visualize the pyramidalization of the ethylene bond. Red arrows indicate the decay path. [Reprinted with permission from *J. Phys. Chem. C*, 2015, **119**, 2249. Copyright 2015 American Chemical Society.]

geometry in the ground state. Two electronic-structure features are important in this internal conversion (IC) process:

(a) The excitation takes place from a π orbital to a π* orbital with bonding and anti-bonding character, respectively, at the double bond that twists.

(b) Along the evolution towards the CIX after photo-excitation, the ground state is characterized by a biradical structure with unpaired electrons in each carbon atom of the double exocyclic bond. On the other hand, the excited state features an ionic electronic configuration with a carbanion atom.

The electronic-structure features determined for the indoline photoisomerization decay channel have been also found in other molecules with favorable *E*/*Z* photoisomerisations.[112–116]

4.2 Excited-state proton/hydrogen transfers

Molecules or complexes with hydrogen donor and acceptor groups form hydrogen-bond networks. These hydrogen bonds take place between highly electronegative atoms (for example, oxygen and nitrogen) and are very common in biological systems and in solutions with water. Illustrative examples are the Watson–Crick adenine–thymine and guanine–cytosine base pairs.[46] In the excited-state chemistry of these systems, proton transfer might be easily achieved if the excited state implies a

transfer of electron density from the part of the molecule with the hydrogen donor to the region with the hydrogen acceptor. Then, the proton transfer takes place in the same direction to compensate the charge separation. In total, a hydrogen atom is transferred. In this process, a CIX is reached which funnels the system to the ground state either towards the original compound (if the hydrogen moves back to its position) or towards the formation of tautomers (if a second hydrogen is transferred). During the last two decades, the excited-state double proton transfer in the 7-azaindole dimer has been intensively studied. Both stepwise and concerted mechanisms have been proposed in the literature. In 2015, Barbatti and co-workers[117] analyzed in detail the static and dynamic properties of the process giving support to the concerted mechanism. In another study,[118] the 7-azaindole monomer was also studied in clusters with up to five water molecules. Multiple excited-state proton transfer (ESPT) were observed in the dynamics simulations in the femtosecond time scale. In clusters of aldehydes, the hydrogen transfer process was determined by Shemesh *et al.*[119] to be the main intermolecular process in the triplet-state photochemistry of the system. ESPT occurring in an antraquinone *via* water molecules was also proposed as a plausible mechanism explaining the production of photoredox reactions without external oxidants or reductants.[120] In other theoretical works, Barbatti and co-workers[121,122] showed the potential use of the ESPT phenomenon to create two-color fluorescent markers for protein binding sites and the role of ESPT to provide photo-stability to peptide-bonded systems to UV irradiation.

ESPT might take place together with other photo-induced processes mentioned in the present work. For example, Guan *et al.*[123] analyzed how the ESPT and *E*/*Z* photoisomerization mechanisms interact in the same molecule, 2-hydroxyazabenzene. Spörkel *et al.*[124] also showed the coexistence of ESPT and photoisomerizations at both C=C and C=N double bonds in a minimal photochromic Schiff base, salicylidene methylamine. Gilch and co-workers[125] explored the sequential channel of ESPT and ring-closure in the photo-reaction from o-acetylbenzaldehyde to 3-methylphthalide.

ESPT is also possible between non-highly electronegative atoms, such as carbon atoms. As shown by Thiel and co-workers,[126] a plausible ESPT channel is present in 2-phenylphenol between oxygen and carbon atoms, which have also been observed experimentally.

4.3 Photodissociations and photocycloadditions

UV-induced dissociation reactions are very important in atmospheric chemistry due to the fact that highly-reactive radical species are formed. In this context, Barbatti and co-workers[127,128] explored in 2014–2015 the energies required to produce halogen atoms in the hydrochlorofluorocarbon $C_2H_2F_3Cl$ and the CH_3OBr atmospheric pollutants. In another study, the O–O bond breaking in the Criegee intermediate CH_2OO to yield either singlet or triplet oxygen was also studied.[129] The Criegee intermediates are formed by the reaction of alkenes from the

biosphere with ozone and can further react with atmospheric species such as H_2O, NO_2, and SO_2. Nitrated polycyclic aromatic hydrocarbons are also an important class of anthropogenic pollutants, mainly produced during the incomplete combustions in vehicles. Giussani[130] performed a CASPT2//CASSCF study on the UV-induced decomposition of the 1-nitronaphthalene. As described by the author, after absorption to the lowest-lying bright states, the most favorable determined process is an ISC towards the lowest-lying triplet state. Next, for the decay to the ground state, Giussani found a second ISC characterized by the formation of an oxaziridine ring. Finally, this cycle can be opened by thermal energy releasing the NO radical. It is worth mentioning that this photochemical reaction might be of interest to remove the pollutant from the atmosphere.

Other types of photodissociation processes that were studied in 2014–2015 are water splitting and photopolymerizations. In the first case, Domcke, Sobolewski, and co-workers explored the potential of hydrogen-bonded complexes between water and aromatic nitro compounds to generate H and OH radicals.[131,132] In the context of excited-state processes of water, it is worth mentioning here the studies reporting distinct spectroscopic properties of water clusters in conformations different than those present in bulk water.[133,134] Regarding the photo-induced polymerization, Huix-Rotllant and Ferre[135] applied quantum chemistry to analyze the mechanism of C–O photo-cleavage in alkoxyamines having an aromatic moiety that absorb light and transfer the excitation energy to the alkoxyamine part. The C–O bond is then weakened and rupture may occur giving rise to a carbon centered radical which can initiate the polymerization.

Finally, we will briefly consider the photoaddition reactions, which might be considered as the photochemical phenomenon opposite to the photo-induced dissociations. A typical example is the $[2+2]$ photocycloaddition in which two adjacent double bonds give rise to a cyclobutane in the excited state. Dolg and co-workers[136] showed that the enantioselectivity of the process in the presence of a chiral oxazaborolidine/AlBr3-based Lewis acid catalyst is due to relativistic effects from the heavy atoms of the catalyst.

4.4 Ring-opening and ring-closure

Photodissociations and photocycloadditions are related to ring-opening and ring-closure reactions, respectively. In the two last processes, the bond breaking/formation takes place in a cyclic compound and therefore the photoreaction does not change the number of fragments. The ring-opening of 1,3-cyclohexadiene to form hexatriene is a case of study since it serves as a model to understand photochemical electrocyclic reactions.[137–139] In 2015 Kim *et al.*[139] extended the *ab initio* multiple spawning method to include field-induced nonadiabatic transitions and showed that the distribution of reactants and products after photoexcitation could be changed by applying a control field. In some cases, the two isomers (open and close forms) can be efficiently interconverted

by means of light, which makes the molecules relevant in the field of molecular rotors. These systems, which photoisomerize between closed and open forms, are so-called Type I compounds, whereas those molecule that undergo *E*/*Z* isomerization of a double bond are known as Type II compounds. In 2014–2015, the dimethyldihydropyrene/cyclophanediene system was studied by computational photochemistry with the objective of providing a deeper comprehension of the mechanism and helping to increase the cycloreversion yields.[140,141]

Cyclic ketones and oligophiophenes are also examples of molecules that present decay channels *via* ring-opening. Cui and co-workers[142] performed a systematic CASPT2//CASSCF study on the deactivation channels of cyclopropanone, cyclobutanone, cyclopentanone, and cyclohexanone, and showed how the CIX responsible for the radiationless decay to the ground state increases its energy upon enlarging the size of the ring. For oligothiophenes, the photodissociation of the C–S bond, and therefore ring-opening, provides a mechanism for IC or ISC back to the ground state. Taking into account the use of these molecules in electronics and photovoltaics, this decay route is an undesirable channel. Theoretical studies have been carried out to determine the electronic-structure features responsible for the ring-opening and how the relaxation channels change upon increasing the number of monomeric units in the oligothiophenes.[143,144]

4.5 Locally-excited *vs.* charge-transfer states

Two common types of excited electronic states are those in which the excitation is localized in a region of the molecule (locally-excited states, LE) and those which imply a transfer of the electron density between two parts of the system (charge transfer states, CT). In certain molecules, both states appear close in energy and compete in the relaxation processes taking place after light absorption. As a consequence of this competition, dual fluorescence might take place. One molecule that has such a feature and that has been intensively studied in the last decade has been 4-(dimethylamino)benzonitrile (DMABN). In 2015, Reguero and co-workers[145] determined the relative energies of the LE and CT states in polar solvents and compared the findings with the relative energy position computed in the 4-aminobenzonitrile molecule, which does not have dual fluorescence. The results of the computations allowed the authors to interpret the distinct experimental observations for the two molecules. Regarding ABN, Reguero, Lasorne and co-workers[146] found a new relaxation path connecting the LE and CT states based on a planar CIX rather than the twisted CIX supported by other groups. Segarra-Martí and Coto[147] studied the 4-(dimethylamino)benzoethyne (DMABE) molecule, which is isoelectronic with DMABN, but does not show dual fluorescence. In contrast to previous studies on DMABN, pronounced energy barriers to reach the CT state were determined, which allowed the authors to rationalize the absence of dual emission in this molecule. Moreover, the role of $\pi\sigma^*$ states in the relaxation mechanism of the dialkylaminobenzonitriles was emphasized. Karasulu and Thiel[148] also studied the

dual fluorescence mechanism, in this case in an electronically modified flavin derivative, roseoflavin. On the basis of the theoretical results, the twisted CT mechanism was suggested as the most favorable one in this molecule.

CT states are also of great interest in organic photovoltaics and in particular in dye-sensitized solar cells. Here, donor–acceptor molecular systems are needed in which the charge transfer state can give rise to two fully dissociated charges. Broer, Havenith, and co-workers[149–151] studied complexes between fullerene derivatives, as electron-acceptors, and distinct donor molecules or polymers to compare their ability to produce efficient charge separation. Ortí and co-workers[152] studied the charge separation process in the fullerene–porphyrin unimolecular system and the effect of π-conjugated molecular bridges.

Furthermore, CT states might be also involved in the singlet fission phenomenon, in which one singlet excited state is converted into two triplet excited states. This process is also of great importance for designing more efficient solar cells.[153–155]

5 Chemiluminescence

Chemiluminescence is the phenomenon of visible light emission promoted by a chemical reaction that has attracted the interest of biologists and chemists for many decades. This thermally-activated chemical reaction produces an intermediate in an excited state which consequently releases energy by light emission. In order to form an electronically excited state, with enough energy to emit visible light, the chemical transformation has to be highly exothermic. A general survey of the phenomenon discloses that, with almost no exception, oxygen is an indispensable reactant in these types of reactions. The reason is that the rupture of peroxide bonds is relatively easy and in the process highly-stable carbonyl compounds are produced. This causes a highly exothermic reaction which leads to the formation of an electronically excited state. The real challenge here lies in understanding in detail how the chemiexcitation occurs from a mechanistic standpoint and how to increase the efficiency of the light emission, for example, by steric enhancement of chemiluminescent compounds.

To be able to explain the mechanism of such chemical reactions, in which various feasible pathways on multiple surfaces compete, one requires methods able to properly compute CIXs and ISCs. It is worth mentioning that DFT and TDDFT methods often produce relatively accurate values for the activation energies and give a good agreement with experimental data. However, since biradical intermediates with several energy-degenerate open-shell electronic configurations play a key role in the chemiluminescence mechanisms, one needs to deal with multiconfigurational problems which requires multi-reference computational methodologies for an accurate description of all the electronic states involved in the process. Therefore, DFT and TDDFT, if properly calibrated, allow a quite good description of the decomposition process on the ground state and the energy location of the lowest triplet.

However, methods of higher accuracy are required to treat the state crossings.[156] The CASPT2//CASSCF protocol is one of the methodologies that can accurately determine CIXs and ISCs points since it accounts both for dynamic and static correlation.

In the period 2014–2015, we found a few theoretical works on chemiluminescence. Among the whole list, we would like to start by reviewing some of them on the parent 1,2-dioxetane molecule. Despite seemingly simple, the decomposition mechanism of this system is complex enough to require the use of high-level methodologies. This peroxidic compound is a common intermediate structure in chemi- and bioluminescence transformations. It possesses high energy content due to the extremely strained four-membered ring and its cleavage leads to stable carbonyl compounds. Previous theoretical studies on the unimolecular decomposition of 1,2-dioxetane indicated the occurrence of a biradical rather than a concerted reaction mechanism.[157] In the biradical mechanism, once the O–O bond is broken, the molecule enters an entropic trapping region of biradical nature in which four singlet and four triplet states are degenerated. After that, the C–C rupture comes into action. One important property to provide with a deeper understanding of the mechanism is the time that 1,2-dioxetane takes to pass through the entropic trapping region before the thermal decomposition. A lower-bound estimation of $\sim$600 fs was computed by Farahani *et al.*[157] by performing CASSCF dynamic simulations on the ground state surface from the TS related to the O–O bond breaking. More accurate estimations would require, however, taking into account the hopping between the degenerated singlet and triplet states. In 2015, Schapiro *et al.*[158] revisited the photo-induced O–O dissociation of the 1,2-dioxetane in order to benchmark their implemented surface hopping algorithm for determining photochemical reaction paths. The advantage of this algorithm is that it evaluates the ''probability'' of hopping to the close-lying surface along the MEP and when it is significant, the MEP is followed on the lower-energy surface. In more technical words, the system does not get stuck into a root-flipping point along the reaction path (MEP) calculation. For dioxetane-like systems, the MEP computation was started on the S_1 state at the reactant geometry. Then, the hopping took place once the system entered the region of degeneracy between the four singlet states (Fig. 16). After that, the molecule is trapped and a redistribution of the energy among the other vibrational modes is required to fragment the molecule to the products.

Another theoretical study on 1,2-dioxetane was performed by West *et al.*[159] The authors proved that the analysis of the quasi-atomic orbitals is able to elucidate any change in bonding pattern that occurs throughout the MEP.

The enhancement of the light emission is another challenge in the engineering of chemiluminescent processes. In the last decades, significant theoretical and experimental efforts have been dedicated to discover and utilize more efficient chemiluminescent substrates for the development of clinical, biological, environmental, or even forensic applications. Here, a well-known chemiluminescence transformation is

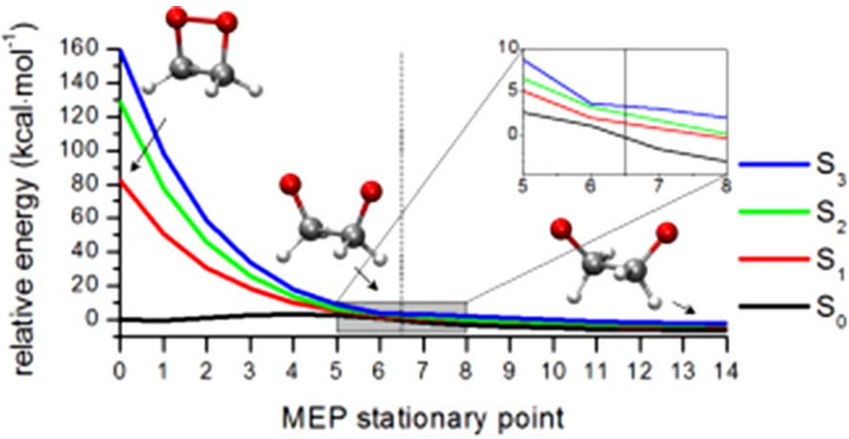

Fig. 16 Non-adiabatic MEP computed for 1,2-dioxetane on the S_1 state (see text). [Adapted from *J. Comput. Chem.*, 2015, **36**, 312–320, with permission from John Wiley and Sons. © 2015 Wiley Periodicals, Inc.]

the oxidation of luminol (5-amino-2,3,dihydro-1,4-phthalazinedione). In the presence of transition metals, the chemiluminescence of luminol can be catalyzed and hence, be more effective. The study of luminol derivatives may give a new insight in a deeper understanding of the non-adiabatic process and their application in a vast number of chemical and biological tissues. Griesbeck *et al.*[156] reported a steric gearing effect on surface crossings in alkyl-substituted luminol. By performing TDDFT and CASPT2//CASSCF calculations, the authors analyzed mechanistic aspects of the chemi-excitation processes for the luminol derivatives and compared the findings with those obtained for the parent luminol. The general mechanism arisen from this study corresponds to a reaction with a small barrier to the TS related to the weak O–O rupture (TS^{O-O}), from which a CIX between S_0 and S_1 surfaces allows the excited-state population (Fig. 17). While TDDFT shows no evidence crossing points, the CASPT2//CASSCF level is in agreement with the experimental observations. The findings imply that the CIX is more accessible for the diethyl derivative than for the parent luminol due to the fact that, in the former molecule, the energy position of the CIX is closer to the energy of the TS^{O-O}. As described by the authors, this implies a more favorable energetic accessibility of the CIX in the diethyl derivative, which facilitates the excited state population. This allows to interpret the higher chemiluminescence yields measured experimentally for the diethyl luminol with respect to the parent molecule. The so-called ''steric gearing'' effect of the ethyl groups can be applied to improve the efficiency of chemiluminescence processes.

6 Dark photochemistry

In the early 70s, the paradoxical hypothesis of ''photochemistry without light'' captured the scientists' attention. The term refers to the fact that photo-induced processes can be produced without irradiating by light.[160]

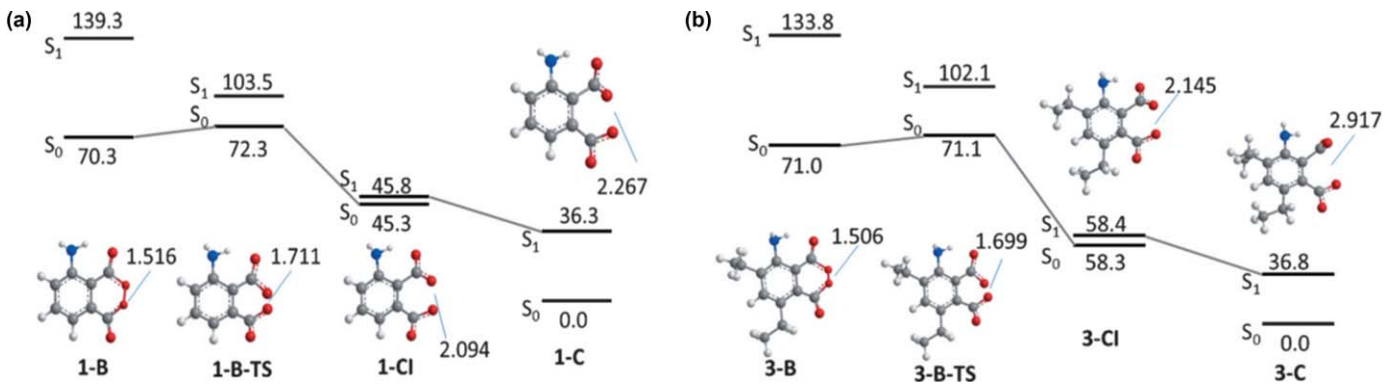

Fig. 17 Critical points of the PES, computed at the CASCPT2//CASSCF for (a) parent luminol and (b) luminol's diethyl derivative. Energies are in kcal mol^{-1} and bond distances in Å. [Reprinted from *Chem. – Eur. J.*, 2015, **21**, 9975, with permission from John Wiley and Sons. © 2015 WILEY-VCH Verlag GmbH & Co. KGaA, Weinheim.]

Instead of light, a chemical reaction is used to form the electronically excited state. Such phenomena might be relevant for bio-organisms living in caves or in the deep sea and it might have interesting applications in technology to produce excited-state chemistry in the darkness.

The molecular basis of this unconventional type of excited-state chemistry was established theoretically by Farahani *et al.*[161] through the study of the thermal decomposition of Dewar dioxetane. This molecule is a combination of 1,2-dioxetane and 1,3-butadiene, which was first presented by McCapra[162] in the study of the thermal decomposition of Dewar benzene. The author observed light emission in this process and it was shown to depend on the presence of oxygen. Thus, the Dewar dioxetane was suggested to be formed in this process and to be responsible for the luminescence. In the theoretical study by Farahani *et al.*,[161] the CASPT2//CASSCF method was employed to characterize the PESs of the lowest-lying singlet and triplet states along the decomposition coordinates on the S_0, S_1 and T_1 manifolds. An initial O–O bond breaking and subsequent C–C cleavage *via* a two-step biradical mechanism was determined as the reaction pathway for the thermal decomposition of the Dewar dioxetane. The findings for the dissociation on S_0 and S_1 were found to be similar to those of 1,2-dioxetane. However, a distinct pattern was determined for T_1. Thus, whereas in 1,2-dioxetane a minimum structure on the T_1 PES was computed along the MEP after the C–C dissociation, in Dewar dioxetane the equivalent MEP reveals a torsion of one of the C=C bonds of the cycle and an evolution towards a singlet-triplet crossing (STC) with the ground state (see Fig. 18). This is caused by an adiabatic transformation between the $n\pi^*$ and $\pi\pi^*$ diabatic states which does not take place in 1,2-dioxetane. From the STC crossing, the system gives rise to two isomers *E* and *Z*, which are the products of the ''photo''-isomerization.

By means of combining 1,2-dioxetane and 1,3-butadiene in Dewar dioxetane and performing thermal dissociation of the resulting compound, one can clearly see the manifestation of a *E*/*Z* isomerization along the T_1 PES and hence, photochemistry without light. As described above by Farahani *et al.*,[161] the dissociation along the triplet manifold brings the reactivity on the excited-state region of butadiene, due to the coupling between the $n\pi^*$ triplet diabatic state and a low-lying $\pi\pi^*$ diabatic state. These findings give an insight to better understand the reported occurrence of photo-metabolites in dark tissues of plants and animals that, according to the Woodward-Hoffman rules, cannot be formed by thermal reactions on the ground state manifold.[160]

7 Bioluminescence

Theoretical studies on bioluminescence generally employ the quantum mechanics (QM) method to investigate the related chemical reactions, the combined QM and molecular mechanics (MM) method to calculate the spectra, the molecular dynamics (MD) to consider the protein fluctuation, the nonadiabatic MD (NAMD) to evaluate the quantum yield of light emitters, and sometimes *ab initio* MD (AIMD) on small model

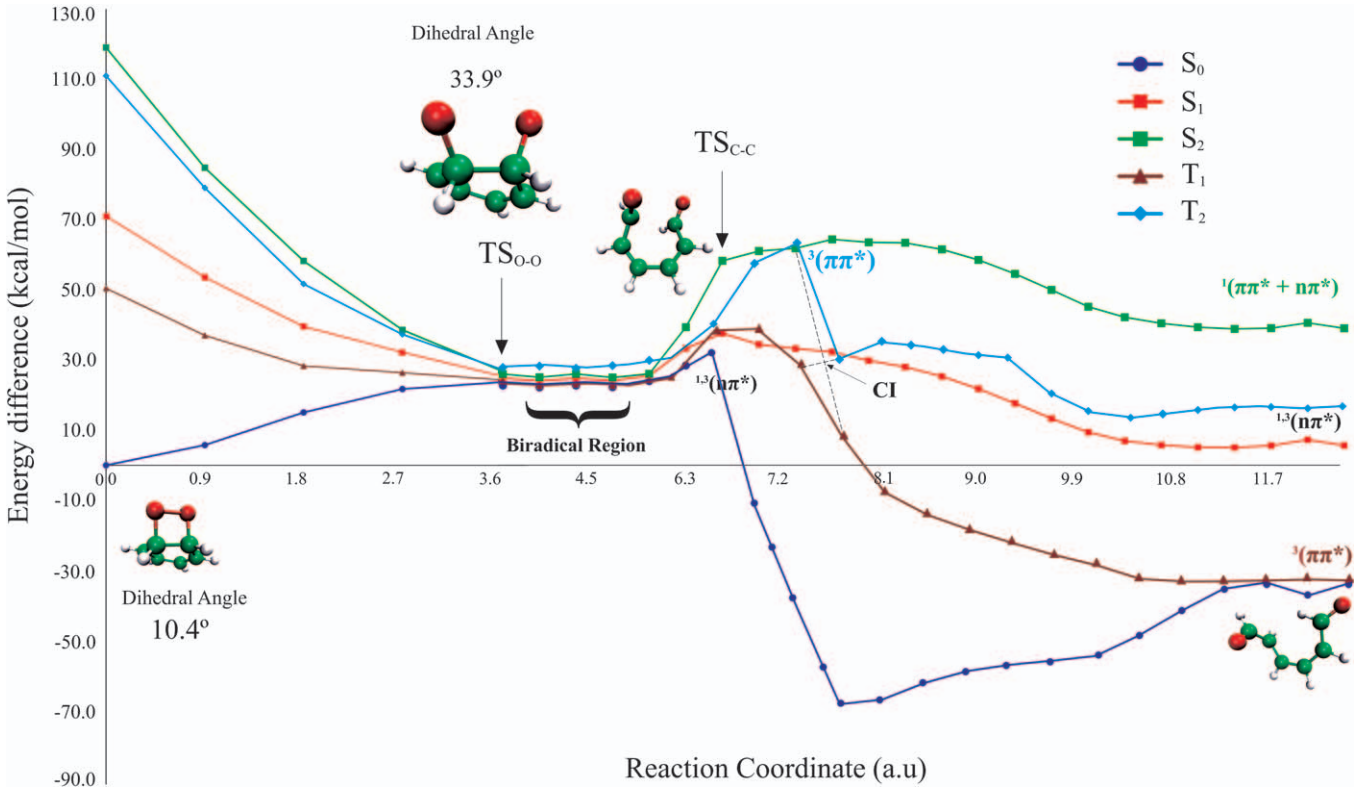

Fig. 18 Decomposition mechanism of Dewar dioxetane. Reported energies are computed at the CASPT2 level of theory. [Adapted from *Phys. Chem. Chem. Phys.*, 2015, **17**, 18653, with permission from the Physical Chemistry Chemical Physics Owner Societies.]

systems to discuss the bioluminescence mechanism. The chemical structures of luciferins and the X-ray structures of luciferase are prerequisite to theoretical research of bioluminescence. Actually, both of them are very limited, compared with the numerous bioluminescent systems in the nature. The years 2014 and 2015 have seen the reports of theoretical studies of firefly,[163–171] *Cypridina*,[172,173] bacteria,[174,175] and obelin.[176] The impressive contributions are briefly summarized below.

What is the exact chemical form of the light emitter of a firefly? This question has been inquired since before the 1960s. There is no doubt that the first singlet excited-state (S_1) oxyluciferin is the light emitter. However, oxyluciferin has six possible chemical forms (keto, enol, keto-1, enol-1, enol-1′, and enol-2, see Fig. 19). Which one or which ones are the light emitter/s of wild firefly has remained unresolved for decades. A recent study[163] provides the solution to the problem *via* QM/MM calculations combined with MD simulations. Those calculations were performed in the real protein for the six chemical forms of oxyluciferin and the corresponding analogues (see Fig. 19).[177] By considering the real environment, the pH value, and a possible equilibrium of the chemical forms of oxyluciferin *in vivo*, the calculated results indicated that the main emitter of the wild firefly is the keto-1 form in its S_1 state.

For the first time, the bioluminescent efficiency was theoretically estimated *via* a NAMD simulation.[178] The chemical origin of the firefly bioluminescence is the thermolysis of firefly dioxetanone anion (FDO^-). A NAMD simulation under the framework of the trajectory surface hopping method was performed on the chemiluminescent decomposition of FDO^-. The theoretical quantum yield of chemiexcitation was estimated to be 39% by counting the number of the trajectories on the energy surfaces of the ground (S_0) and the S_1 states. Using the experimental fluorescent quantum yield (62%) of the oxyluciferin analogue, the overall chemiluminescent efficiency in the keto-1 decomposition was approximately estimated to be 24%, which is in agreement with experimental measurements.

Regarding the mechanism of *Cypridina* bioluminescence, it is worth mentioning first that *Cypridina hilgendorfii* is a bioluminescent crustacean whose bioluminescence reaction is archetypal for a number of marine organisms, which highlight the relevance of the system. As described in Fig. 20, *Cypridina* produces light in a three-step reaction. First, the cypridinid luciferin is activated by an enzyme to produce a peroxide intermediate, cypridinid dioxetanone (CDO), which then decomposes to generate the S_1-state of the oxyluciferin (OxyCLnH*). Finally, OxyCLnH* de-excites to its S_0 state along with emission of bright blue light. The detailed mechanism remained unknown, and especially it was unclear whether the light emitter is generated from a neutral form (CDOH) or anionic form (CDO^-) of the CDO precursor. Hence, the recent work[172] investigated this key step. The calculated results indicate that the decomposition of CDO^- occurs *via* the gradually reversible charge transfer initiated luminescence mechanism, whereas CDOH decomposes through an entropic trapping mechanism. The thermolysis of CDO^- produces the S_1 state of the oxyluciferin anion ($OxyCLn^{-}$*),

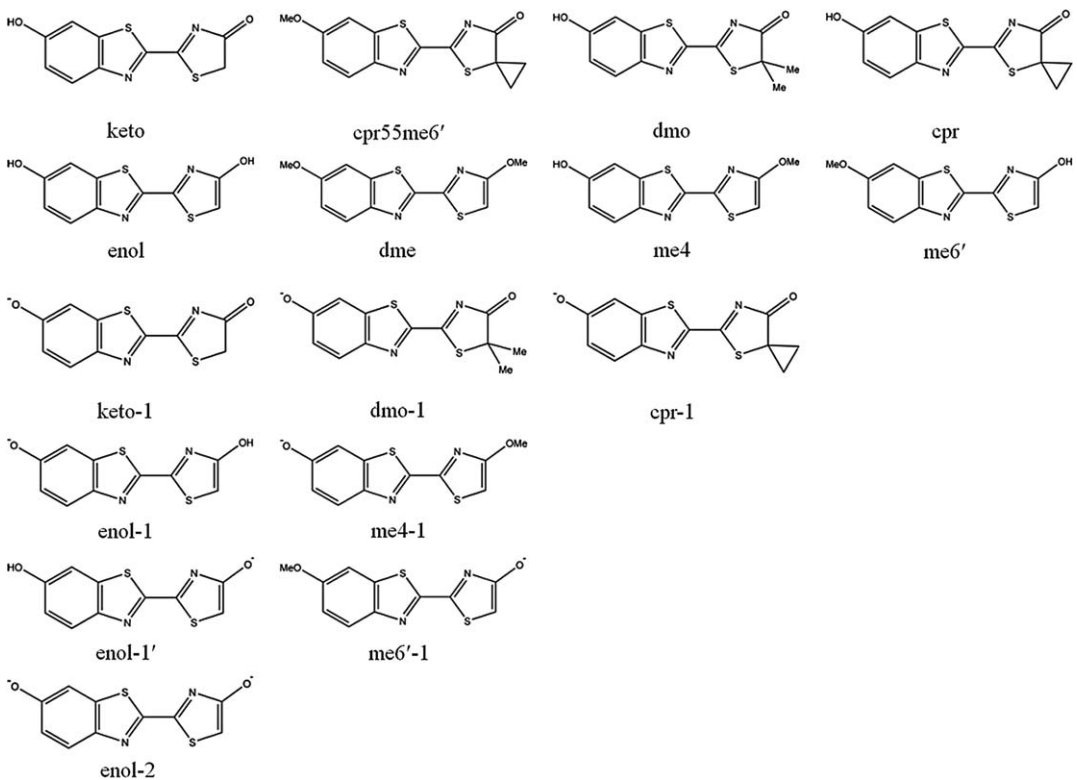

Fig. 19 Molecular structures of the six possible chemical forms of firefly oxyluciferin and the corresponding analogues.

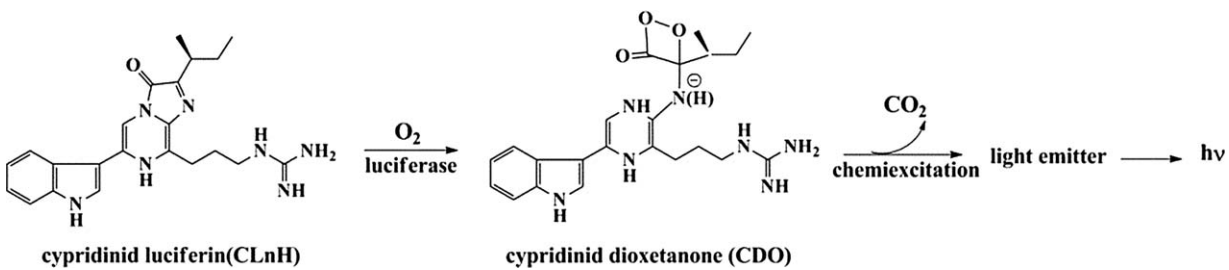

Fig. 20 Simplified three-step reaction mechanism proposed for *Cypridina* bioluminescence.

which combines with a proton from the environment to form OxyCLnH*, the actual light emitter for the natural system.

Finally, bacterial bioluminescence has got important applications in water-quality monitoring and *in vivo* imaging, but its bioluminescent mechanism was also largely unknown. In 2014, the entire process of bacterial bioluminescence, from the whole chemical reaction channel to light emission was investigated by using QM, QM/MM, and MD calculations in the gas phase, as well as solvent and protein environments.[175] This investigation revealed that: (a) the key step of the bioluminescent process, decomposition of flavinperoxyhemiacetal, occurs according to the charge-transfer initiated luminescence mechanism and (b) the first excited state of 4*a*-hydroxy-4*a*,5-dihydro flavin mononucleotide was affirmed to be the bioluminophore of bacterial bioluminescence. These conclusions were further confirmed by following higher-level calculations.[174]

8 Summary

In the present chapter, we have reviewed the advances in computational photochemistry and chemiluminescence in 2014 and 2015 assembling them in the categories of method developments, dynamics, mechanisms of DNA/RNA damage, photochemical phenomena in bio- and nano-molecules, and excited-state chemistry initiated by a thermal reaction.

Recent trends in theory development corresponds to improvements of density functional theory (DFT) methods to correctly treat conical intersections (CIXs), assessment of approximate methods in describing the CIX, finding CIXs in solution, improved treatment of time dependent DFT for Rydberg states, the use of frozen natural orbitals in conjunction with the multi-configurational second order perturbation theory, and combination of multiconfigurational wave function theory with DFT for ground and excited states. Regarding the advances in dynamic approaches, recent works focus on methods using local control theory to select the product of the interaction between a molecule and light, how to include tunnelling in semi-classical simulations of non-adiabatic reactions, the use of symmetrical windowing for quantum states in semi-classical techniques, improved and simple methods for diabatizations, and the use of Smolyak's technique in dynamical simulations.

In 2014–2015, application of theory in computational photochemistry and chemiluminescence has allowed a deeper comprehension of the mechanisms of DNA interaction with UV light, reactive oxygen species, low-energy electrons, and other exogenous and endogenous species. In addition, new and relevant findings have been obtained related to *E*/*Z* photoisomerizations, excited-state proton/hydrogen transfers, photodissociations/photocycloadditions, ring-opening/closure processes, and phenomena involving locally-excited/charge transfer states. Furthermore, the mechanisms of chemically-initiated light emission (chemiluminescence and bioluminescence) and chemically-induced excited-state processes (dark photochemistry) have been deeply analyzed.

Acknowledgements

Research supported by the Spanish *Ministerio de Economía y Competitividad/Fondo Europeo de Desarrollo Regional* (MINECO/FEDER) (Project No. CTQ2014-58624-P and *Juan de la Cierva* Grant No. JCI-2012-13431), the Swedish Research Council (Grant No. 2012-3910), the eSSENCE program, the Uppsala University, the *Fundação de Amparo á Pesquisa do Estado de São Paulo* (FAPESP) (Project No. 2015/02314-8) and the National Nature Science Foundation of China (Grant No. 21325312).

References

1 Resolution Number 68/221, 68th Session of the General Assembly of the United Nations, United Nations, December 2013.
2 The Nobel Prize in Chemistry 2015, http://www.nobelprize.org/nobel_prizes/chemistry/laureates/2015/, (accessed April 2016).
3 L. Serrano-Andrés, D. Roca-Sanjuán and G. Olaso-González, in *Photochemistry*, ed. A. Albini, Royal Society of Chemistry, London, 2010, vol. 38, pp. 10–36.
4 Y.-J. Liu, D. Roca-Sanjuán and R. Lindh, in *Photochemistry*, ed. A. Albini, Royal Society of Chemistry, London, 2012, vol. 40, p. 42.
5 D. Roca-Sanjuán, I. Fdez. Galván, R. Lindh and Y.-J. Liu, in *Photochemistry*, ed. E. Fasani and A. Albini, Royal Society of Chemistry, London, 2015, vol. 42, p. 11.
6 S. L. Li, A. V. Marenich, X. Xu and D. G. Truhlar, *J. Phys. Chem. Lett.*, 2014, **5**, 322.
7 A. Nikiforov, J. A. Gamez, W. Thiel, M. Huix-Rotllant and M. Filatov, *J. Chem. Phys.*, 2014, **141**, 124122.
8 N. Minezawa, *J. Chem. Phys.*, 2014, **141**, 164118.
9 G. Li Manni, R. K. Carlson, S. Luo, D. Ma, J. Olsen, D. G. Truhlar and L. Gagliardi, *J. Chem. Theory Comput.*, 2016, **12**, 458.
10 S. Ghosh, A. L. Sonnenberger, C. E. Hoyer, D. G. Truhlar and L. Gagliardi, *J. Chem. Theory Comput.*, 2015, **11**, 3643.
11 J. Segarra-Martí, M. Garavelli and F. Aquilante, *J. Chem. Theory Comput.*, 2015, **11**, 3772.
12 S. L. Li and D. G. Truhlar, *J. Chem. Theory Comput.*, 2015, **11**, 3123.
13 J. Zheng, X. Xu, R. Meana-Paneda and D. G. Truhlar, *Chem. Sci.*, 2014, **5**, 2091.
14 S. Nangia, A. W. Jasper, T. F. Miller and D. G. Truhlar, *J. Chem. Phys.*, 2004, **120**, 3586.
15 J. Zheng, R. Meana-Paneda and D. G. Truhlar, *J. Phys. Chem. Lett.*, 2014, **5**, 2039.
16 K. R. Yang, X. Xu and D. G. Truhlar, *Chem. Phys. Lett.*, 2013, **573**, 84.
17 G. J. Atchity and K. Ruedenberg, *Theor. Chem. Acc.*, 1997, **97**, 47.
18 S. L. Li, D. G. Truhlar, M. W. Schmidt and M. S. Gordon, *J. Chem. Phys.*, 2015, **142**, 1.
19 B. F. E. Curchod, T. J. Penfold, U. Rothlisberger and I. Tavernelli, *Phys. Rev. A: At., Mol., Opt. Phys.*, 2011, **84**, 042507.
20 B. F. E. Curchod, T. J. Penfold, U. Rothlisberger and I. Tavernelli, *ChemPhysChem*, 2015, **16**, 2127.
21 S. J. Cotton and W. H. Miller, *J. Phys. Chem. A*, 2013, **117**, 7190.

22 S. J. Cotton, K. Igumenshchev and W. H. Miller, *J. Chem. Phys.*, 2014, **141**, 0841004.
23 J. Nance and C. T. Kelley, *SIAM J. Sci. Comput.*, 2015, **37**, S137–S156.
24 S. Maeda, T. Taketsugu, K. Ohno and K. Morokuma, *J. Am. Chem. Soc.*, 2015, **137**, 3433.
25 S. Mai, P. Marquetand and L. González, *Int. J. Quantum Chem.*, 2015, **115**, 1215.
26 F. Levi, S. Mostarda, F. Rao and F. Mintert, *Rep. Prog. Phys.*, 2015, **78**, 082001.
27 J. P. Malhado, M. J. Bearpark and J. T. Hynes, *Front. Chem.*, 2014, **2**, 97.
28 M. Persico and G. Granucci, *Theor. Chem. Acc.*, 2014, **133**, 1040.
29 M. Wormit, D. R. Rehn, P. H. P. Harbach, J. Wenzel, C. M. Krauter, E. Epifanovsky and A. Dreuw, *Mol. Phys.*, 2014, **112**, 774.
30 L. Blancafort, *ChemPhysChem*, 2014, **15**, 3166.
31 F. P. Noonan, M. R. Zaidi, A. Wolnicka-Glubisz, M. R. Anver, J. Bahn, A. Wielgus, J. Cadet, T. Douki, S. Mouret, M. A. Tucker, A. Popratiloff, G. Merlino and E. C. De Fabo, *Nat. Commun.*, 2012, **3**, 884.
32 A. Giussani, J. Segarra-Martí, D. Roca-Sanjuán and M. Merchán, *Top. Curr. Chem.*, 2015, **355**, 57.
33 S. Mai, M. Richter, P. Marquetand and L. González, *Top. Curr. Chem.*, 2015, **355**, 99.
34 R. Improta, F. Santoro and L. Blancafort, *Chem. Rev.*, 2016, **116**, 3540.
35 L. Blancafort and A. A. Voityuk, *J. Chem. Phys.*, 2014, **140**, 18A301.
36 R. R. Ramazanov, D. A. Maksimov and A. I. Kononov, *J. Am. Chem. Soc.*, 2015, **137**, 11656.
37 M. Barbatti, *J. Am. Chem. Soc.*, 2014, **136**, 10246.
38 D. Tuna, A. L. Sobolewski and W. Domcke, *J. Phys. Chem. A*, 2014, **118**, 122.
39 R. Szabla, J. Campos, J. E. Sponer, J. Sponer, R. W. Gora and J. D. Sutherland, *Chem. Sci.*, 2015, **6**, 2035.
40 B. P. Fingerhut, K. E. Dorfman and S. Mukamel, *J. Chem. Theory Comput.*, 2014, **10**, 1172.
41 F. J. Avila Ferrer, F. Santoro and R. Improta, *Comput. Theor. Chem.*, 2014, **1040**, 186.
42 I. Conti, A. Nenov, S. Hoefinger, S. F. Altavilla, I. Rivalta, E. Dumont, G. Orlandi and M. Garavelli, *Phys. Chem. Chem. Phys.*, 2015, **17**, 7291.
43 M. Barbatti, *ChemPhysChem*, 2014, **15**, 3342.
44 S. Yuan, H. Hong, G. Wang, W. Zhang, Y. Dou and G. V. Lo, *Int. J. Photoenergy*, 2014, 1.
45 H. Wang, X. Chen and W. Fang, *Phys. Chem. Chem. Phys.*, 2014, **16**, 25432.
46 A. Francés-Monerris, J. Segarra-Martí, M. Merchán and D. Roca-Sanjuán, *Theor. Chem. Acc.*, 2016, **135**, 31.
47 K. Rottger, H. J. B. Marroux, M. P. Grubb, P. M. Coulter, H. Bohnke, A. S. Henderson, M. C. Galan, F. Temps, A. J. Orr-Ewing and G. M. Roberts, *Angew. Chem., Int. Ed.*, 2015, **54**, 14719.
48 W. Lee and S. Matsika, *Phys. Chem. Chem. Phys.*, 2015, **17**, 9927.
49 I. Rivalta, A. Nenov, G. Cerullo, S. Mukamel and M. Garavelli, *Int. J. Quantum Chem.*, 2014, **114**, 85.
50 A. Nenov, A. Giussani, B. P. Fingerhut, I. Rivalta, E. Dumont, S. Mukamel and M. Garavelli, *Phys. Chem. Chem. Phys.*, 2015, **17**, 30925.
51 A. Nenov, A. Giussani, J. Segarra-Martí, V. K. Jaiswal, I. Rivalta, G. Cerullo, S. Mukamel and M. Garavelli, *J. Chem. Phys.*, 2015, **142**, 212443.

52 A. Nenov, J. Segarra-Martí, A. Giussani, I. Conti, I. Rivalta, E. Dumont, V. K. Jaiswal, S. F. Altavilla, S. Mukamel and M. Garavelli, *Faraday Discuss.*, 2015, **177**, 345.
53 M. Pollum, L. Martínez-Fernández and C. E. Crespo-Hernandez, *Top. Curr. Chem.*, 2015, **355**, 245.
54 Z. Lu, A. A. Beckstead, B. Kohler and S. Matsika, *J. Phys. Chem. B*, 2016, **120**, 597.
55 D. Tuna and W. Domcke, *Phys. Chem. Chem. Phys.*, 2016, **18**, 947.
56 J. Rak, L. Chomicz, J. Wiczk, K. Westphal, M. Zdrowowicz, P. Wityk, M. Zyndul, S. Makurat and L. Golon, *J. Phys. Chem. B*, 2015, **119**, 8227.
57 M. P. Burke, K. M. Borland and V. A. Litosh, *Curr. Top. Med. Chem.*, 2016, **16**, 1231.
58 C. S. Foote, *Photochem. Photobiol.*, 1991, **54**, 659.
59 P. Karran and N. Attard, *Nat. Rev. Cancer*, 2008, **8**, 24.
60 E. Kaminskas, A. T. Farrell, Y. C. Wang, R. Sridhara and R. Pazdur, *Oncologist*, 2005, **10**, 176.
61 L. Martínez-Fernández, I. Corral, G. Granucci and M. Persico, *Chem. Sci.*, 2014, **5**, 1336.
62 G. L. Cui and W. Thiel, *J. Phys. Chem. Lett.*, 2014, **5**, 2682.
63 J. P. Gobbo and A. C. Borin, *Comput. Theor. Chem.*, 2014, **1040**, 195.
64 A. Giussani, M. Merchán, J. P. Gobbo and A. C. Borin, *J. Chem. Theory Comput.*, 2014, **10**, 3915.
65 X. Guo, Y. Zhao and Z. Cao, *J. Phys. Chem. A*, 2014, **118**, 9013.
66 M. C. Cuquerella, V. Lhiaubet-Vallet, J. Cadet and M. A. Miranda, *Acc. Chem. Res.*, 2012, **45**, 1558.
67 E. Dumont and A. Monari, *Front. Chem.*, 2015, **3**, 43.
68 M. Huix-Rotllant, E. Dumont, N. Ferre and A. Monari, *Photochem. Photobiol.*, 2015, **91**, 323.
69 D.-C. Sergentu, R. Maurice, R. W. A. Havenith, R. Broer and D. Roca-Sanjuán, *Phys. Chem. Chem. Phys.*, 2014, **16**, 25393.
70 E. Dumont, M. Wibowo, D. Roca-Sanjuán, M. Garavelli, X. Assfeld and A. Monari, *J. Phys. Chem. Lett.*, 2015, **6**, 576.
71 J. J. Nogueira, M. Oppel and L. González, *Angew. Chem., Int. Ed.*, 2015, **54**, 4375.
72 M. Jaeger, L. Freitag and L. González, *Coordin. Chem. Rev.*, 2015, **304**, 146.
73 C. Mari, V. Pierroz, S. Ferrari and G. Gasser, *Chem. Sci.*, 2015, **6**, 2660.
74 C. Reichardt, M. Pinto, M. Waechtler, M. Stephenson, S. Kupfer, T. Sainuddin, J. Guthmuller, S. A. McFarland and B. Dietzek, *J. Phys. Chem. A*, 2015, **119**, 3986.
75 L. Freitag and L. González, *Inorg. Chem.*, 2014, **53**, 6415.
76 M. E. Alberto, B. C. De Simone, G. Mazzone, E. Sicilia and N. Russo, *Phys. Chem. Chem. Phys.*, 2015, **17**, 23595.
77 M. E. Alberto, B. C. De Simone, G. Mazzone, T. Marino and N. Russo, *Dyes Pigments*, 2015, **120**, 335.
78 L. Martínez-Fernández, J. González-Vazquez, L. González and I. Corral, *J. Chem. Theory Comput.*, 2015, **11**, 406.
79 A. Francés-Monerris, M. Merchán and D. Roca-Sanjuán, *J. Phys. Chem. B*, 2014, **118**, 2932.
80 A. Francés-Monerris, M. Merchán and D. Roca-Sanjuán, *J. Chem. Phys.*, 2013, **139**, 071101.
81 I. Baccarelli, I. Bald, F. A. Gianturco, E. Illenberger and J. Kopyra, *Phys. Rep.*, 2011, **508**, 1.

82 T. Sommerfeld, *J. Phys. Chem. A*, 2004, **108**, 9150.
83 B. D. Michael and P. O'Neill, *Science*, 2000, **287**, 1603.
84 H. Abdoul-Carime, S. Gohlke and E. Illenberger, *Phys. Rev. Lett.*, 2004, **92**, 168103.
85 A. Francés-Monerris, J. Segarra-Martí, M. Merchán and D. Roca-Sanjuán, *J. Chem. Phys.*, 2015, **143**, 215101.
86 M. Micciarelli, M. Valadan, B. Della Ventura, G. Di Fabio, L. De Napoli, S. Bonella, U. Roethlisberger, I. Tavernelli, C. Altucci and R. Velotta, *J. Phys. Chem. B*, 2014, **118**, 4983.
87 M. I. Taccone, G. Feraud, M. Berdakin, C. Dedonder-Lardeux, C. Jouvet and G. A. Pino, *J. Chem. Phys.*, 2015, **143**, 041103.
88 I. Schapiro and S. Ruhman, *Biochim., Biophys., Acta, Bioenerg.*, 2014, **1837**, 589.
89 E. Walczak and T. Andruniow, *Phys. Chem. Chem. Phys.*, 2015, **17**, 17169.
90 I. Rivalta, A. Nenov and M. Garavelli, *Phys. Chem. Chem. Phys.*, 2014, **16**, 16865.
91 I. Rivalta, A. Nenov, O. Weingart, G. Cerullo, M. Garavelli and S. Mukamel, *J. Phys. Chem. B*, 2014, **118**, 8396.
92 M. Di Donato, M. S. Centellas, A. Lapini, M. Lima, F. Avila, F. Santoro, C. Cappelli and R. Righini, *J. Phys. Chem. B*, 2014, **118**, 9613.
93 C. Punwong, J. Owens and T. J. Martínez, *J. Phys. Chem. B*, 2015, **119**, 704.
94 H. L. Luk, F. Melaccio, S. Rinaldi, S. Gozem and M. Olivucci, *P. Natl.Acad. Sci. USA*, 2015, **112**, 15297.
95 S. Rinaldi, F. Melaccio, S. Gozem, F. Fanelli and M. Olivucci, *Abstr. Pap. Am. Chem. Soc.*, 2014, **247**, 477-PHYS.
96 I. Dokukina and O. Weingart, *Phys. Chem. Chem. Phys.*, 2015, **17**, 25142.
97 D. Polli, O. Weingart, D. Brida, E. Poli, M. Maiuri, K. M. Spillane, A. Bottoni, P. Kukura, R. A. Mathies, G. Cerullo and M. Garavelli, *Angew. Chem., Int. Ed.*, 2014, **53**, 2504.
98 L. Wei, H. Wang, X. Chen, W. Fang and H. Wang, *Phys. Chem. Chem. Phys.*, 2014, **16**, 25263.
99 F. Fernández García-Prieto, M. A. Aguilar, I. Fdez. Galván, A. Muñoz-Losa, F. J. Olivares del Valle, M. L. Sánchez and M. E. Martín, *J. Phys. Chem. A*, 2015, **119**, 5504.
100 S. Gozem, F. Melaccio, H. L. Luk, S. Rinaldi and M. Olivucci, *Chem. Soc. Rev.*, 2014, **43**, 4019.
101 D. Hu, J. Huang, Y. Xie, L. Yue, X. Zhuang and Z. Lan, *Chem. Phys.*, 2015, **463**, 95.
102 I. Schapiro, S. Fusi, M. Olivucci, T. Andruniow, S. Sasidharanpillai and G. R. Loppnow, *J. Phys. Chem. B*, 2014, **118**, 12243.
103 G. Marchand, J. Eng, I. Schapiro, A. Valentini, L. M. Frutos, E. Pieri, M. Olivucci, J. Leonard and E. Gindensperger, *J. Phys. Chem. Lett.*, 2015, **6**, 599.
104 M. Filatov and M. Olivucci, *J. Org. Chem.*, 2014, **79**, 3587.
105 D. Martínez-López, M.-L. Yu, C. Garcia-Iriepa, P. J. Campos, L. Manuel Frutos, J. A. Golen, S. Rasapalli and D. Sampedro, *J. Org. Chem.*, 2015, **80**, 3929.
106 F. Knoch, D. Morozov, M. Boggio-Pasqua and G. Groenhof, *Comput. Theor. Chem.*, 2014, **1040**, 120.
107 G. Cui, P.-J. Guan and W.-H. Fang, *J. Phys. Chem. A*, 2014, **118**, 4732.
108 J. A. Gámez, A. Koslowski and W. Thiel, *RSC Adv.*, 2014, **4**, 1886.
109 F. Zapata, M. Angel Fernández-González, D. Rivero, A. Álvarez, M. Marazzi and L. Manuel Frutos, *J. Chem. Theory Comput.*, 2014, **10**, 312.
110 X.-P. Chang, C.-X. Li, B.-B. Xie and G. Cui, *J. Phys. Chem. A*, 2015, **119**, 11488.
111 R. Losantos, M. S. Churio and D. Sampedro, *ChemistryOpen*, 2015, **4**, 155.

112 A. M. El-Zohry, D. Roca-Sanjuán and B. Zietz, *J. Phys. Chem. C*, 2015, **119**, 2249.
113 B. G. Levine and T. J. Martínez, *Annu. Rev. Phys. Chem.*, 2007, **58**, 613.
114 V. Molina, M. Merchán, B. O. Roos and P.-Å. Malmqvist, *Phys. Chem. Chem. Phys.*, 2000, **2**, 2211.
115 J. Quenneville and T. J. Martínez, *J. Phys. Chem. A*, 2003, **107**, 829.
116 G. Tomasello, M. Garavelli and G. Orlandi, *Phys. Chem. Chem. Phys.*, 2013, **15**, 19763.
117 R. Crespo-Otero, N. Kungwan and M. Barbatti, *Chem. Sci.*, 2015, **6**, 5762.
118 N. Kungwan, K. Kerdpol, R. Daengngern, S. Hannongbua and M. Barbatti, *Theor. Chem. Acc.*, 2014, **133**, 1480.
119 D. Shemesh, S. L. Blair, S. A. Nizkorodov and R. B. Gerber, *Phys. Chem. Chem. Phys.*, 2014, **16**, 23861.
120 J. Dai, J. Han, X. Chen, W. Fang, J. Ma and D. L. Phillips, *Phys. Chem. Chem. Phys.*, 2015, **17**, 27001.
121 D. T. Mancini, K. Sen, M. Barbatti, W. Thiel and T. C. Ramalho, *ChemPhysChem*, 2015, **16**, 3444.
122 R. Crespo-Otero, A. Mardykov, E. Sanchez-Garcia, W. Sander and M. Barbatti, *Phys. Chem. Chem. Phys.*, 2014, **16**, 18877.
123 P.-J. Guan, G. Cui and Q. Fang, *ChemPhysChem*, 2015, **16**, 805.
124 L. Spörkel, J. Jankowska and W. Thiel, *J. Phys. Chem. B*, 2015, **119**, 2702.
125 S. Froebel, L. Buschhaus, T. Villnow, O. Weingart and P. Gilch, *Phys. Chem. Chem. Phys.*, 2015, **17**, 376.
126 S.-H. Xia, B.-B. Xie, Q. Fang, G. Cui and W. Thiel, *Phys. Chem. Chem. Phys.*, 2015, **17**, 9687.
127 L. Stojanovic, G. P. Rodrigues, S. G. Aziz, R. H. Hilal and M. Barbatti, *RSC Adv.*, 2015, **5**, 97003.
128 G. P. Rodrigues, E. Ventura, S. A. do Monte and M. Barbatti, *J. Phys. Chem. A*, 2014, **118**, 12041.
129 R. Dawes, B. Jiang and H. Guo, *J. Am. Chem. Soc.*, 2015, **137**, 50.
130 A. Giussani, *J. Chem. Theory Comput.*, 2014, **10**, 3987.
131 X. Liu, A. L. Sobolewski and W. Domcke, *J. Phys. Chem. A*, 2014, **118**, 7788.
132 X. Liu, T. N. V. Karsili, A. L. Sobolewski and W. Domcke, *J. Phys. Chem. B*, 2015, **119**, 10664.
133 J. Segarra-Martí, D. Roca-Sanjuán and M. Merchán, *Comput. Theor. Chem.*, 2014, **1040**, 266.
134 J. Segarra-Martí, D. Roca-Sanjuán and M. Merchán, *Entropy*, 2014, **16**, 4101.
135 M. Huix-Rotllant and N. Ferre, *J. Phys. Chem. A*, 2014, **118**, 4464.
136 H. Wang, X. Cao, X. Chen, W. Fang and M. Dolg, *Angew. Chem., Int. Ed.*, 2015, **54**, 14295.
137 A. Ohta, O. Kobayashi, S. O. Danielache and S. Nanbu, *Chem. Phys.*, 2015, **459**, 45.
138 C. C. Pemberton, Y. Zhang, K. Saita, A. Kirrander and P. M. Weber, *J. Phys. Chem. A*, 2015, **119**, 8832.
139 J. Kim, H. Tao, T. J. Martínez and P. Bucksbaum, *J. Phys. B: At., Mol. Opt. Phys.*, 2015, **48**, 164003.
140 M. Boggio-Pasqua and M. Garavelli, *J. Phys. Chem. A*, 2015, **119**, 6024.
141 D. Roldan, S. Cobo, F. Lafolet, N. Vila, C. Bochot, C. Bucher, E. Saint-Aman, M. Boggio-Pasqua, M. Garavelli and G. Royal, *Chem. – Eur. J.*, 2015, **21**, 455.
142 S.-H. Xia, X.-Y. Liu, Q. Fang and G. Cui, *J. Phys. Chem. A*, 2015, **119**, 3569.
143 D. Fazzi, M. Barbatti and W. Thiel, *Phys. Chem. Chem. Phys.*, 2015, **17**, 7787.

144 P. Koelle, T. Schnappinger and R. de Vivie-Riedle, *Phys. Chem. Chem. Phys.*, 2016, **18**, 7903.
145 I. Gómez, P. J. Castro and M. Reguero, *J. Phys. Chem. A*, 2015, **119**, 1983.
146 A. Perveaux, P. J. Castro, D. Lauvergnat, M. Reguero and B. Lasorne, *J. Phys. Chem. Lett.*, 2015, **6**, 1316.
147 J. Segarra-Martí and P. B. Coto, *Phys. Chem. Chem. Phys.*, 2014, **16**, 25642.
148 B. Karasulu and W. Thiel, *J. Phys. Chem. B*, 2015, **119**, 928.
149 H. D. de Gier, R. Broer and R. W. A. Havenith, *Proc. SPIE*, 2015, **9567**, 95670N.
150 H. D. de Gier, B. J. Rietberg, R. Broer and R. W. A. Havenith, *Comput. Theor. Chem.*, 2014, **1040**, 202.
151 H. D. de Gier, R. Broer and R. W. A. Havenith, *Phys. Chem. Chem. Phys.*, 2014, **16**, 12454.
152 B. Pelado, F. Abou-Chahine, J. Calbo, R. Caballero, P. de la Cruz, J. M. Junquera-Hernández, E. Ortí, N. V. Tkachenko and F. Langa, *Chem. – Eur. J.*, 2015, **21**, 5814.
153 O. Varnavski, N. Abeyasinghe, J. Arago, J. J. Serrano-Pérez, E. Ortí, J. T. López Navarrete, K. Takimiya, D. Casanova, J. Casado and T. Goodson, III, *J. Phys. Chem. Lett.*, 2015, **6**, 1375.
154 P. B. Coto, S. Sharifzadeh, J. B. Neaton and M. Thoss, *J. Chem. Theory Comput.*, 2015, **11**, 147.
155 J. Zirzlmeier, D. Lehnherr, P. B. Coto, E. T. Chernick, R. Casillas, B. S. Basel, M. Thoss, R. R. Tykwinski and D. M. Guldi, *Proc. Natl. Acad. Sci. U. S. A.*, 2015, **112**, 5325.
156 A. G. Griesbeck, Y. Diaz-Miara, R. Fichtler, A. Jacobi von Wangelin, R. Pérez-Ruiz and D. Sampedro, *Chem. – Eur. J.*, 2015, **21**, 9975.
157 P. Farahani, D. Roca-Sanjuán, F. Zapata and R. Lindh, *J. Chem. Theory Comput.*, 2013, **9**, 5404.
158 I. Schapiro, D. Roca-Sanjuán, R. Lindh and M. Olivucci, *J. Comput. Chem.*, 2015, **36**, 312.
159 A. C. West, M. W. Schmidt, M. S. Gordon and K. Ruedenberg, *J. Phys. Chem. A*, 2015, **119**, 10376.
160 W. J. Baader, C. V. Stevani and E. J. H. Bechara, *J. Brazil. Chem. Soc.*, 2015, **26**, 2430.
161 P. Farahani, M. Lundberg, R. Lindh and D. Roca-Sanjuán, *Phys. Chem. Chem. Phys.*, 2015, **17**, 18653.
162 F. McCapra, *Pure Appl. Chem.*, 1970, **24**, 611.
163 Y.-Y. Cheng and Y.-J. Liu, *J. Chem. Theory Comput.*, 2015, **11**, 5360.
164 Y. Y. Cheng, J. Zhu and Y. J. Liu, *Chem. Phys. Lett.*, 2014, **591**, 156.
165 L. P. da Silva and J. da Silva, *J. Phys. Chem. B*, 2015, **119**, 2140.
166 L. P. da Silva and J. da Silva, *Chem. Phys. Lett.*, 2014, **608**, 45.
167 L. P. da Silva and J. C. G. Esteves da Silva, *ChemPhysChem*, 2014, **16**, 455.
168 M. Hiyama, Y. Noguchi, H. Akiyama, K. Yamada and N. Koga, *Photochem. Photobiol.*, 2015, **91**, 819.
169 Y. Noguchi, M. Hiyama, H. Akiyama and N. Koga, *J. Chem. Phys.*, 2014, **141**, 044309.
170 O. V. Maltsev, L. Yue, M. Rebarz, L. Hintermann, M. Sliwa, C. Ruckebusch, L. Pejov, Y.-J. Liu and P. Naumov, *Chem. – Eur. J.*, 2014, **20**, 10782.
171 H. Sakai and N. Wada, *Comput. Theor. Chem.*, 2014, **1045**, 93.
172 B.-W. Ding, P. Naumov and Y.-J. Liu, *J. Chem. Theory Comput.*, 2015, **11**, 591.

173 Y. Ishii, C. Hayashi, Y. Suzuki and T. Hirano, *Photochem. Photobiol. Sci.*, 2014, **13**, 182.
174 S. Gozem, E. Mirzakulova, I. Schapiro, F. Melaccio, K. D. Glusac and M. Olivucci, *Angew. Chem., Int. Ed.*, 2014, **53**, 9870.
175 C. Hou, Y.-J. Liu, N. Ferre and W.-H. Fang, *Chem. – Eur. J.*, 2014, **20**, 7979.
176 S. Chen, I. Navizet, R. Lindh, Y. Liu and N. Ferre, *J. Phys. Chem. B*, 2014, **118**, 2896.
177 A. Ghose, M. Rebarz, O. V. Maltsev, L. Hintermann, C. Ruckebusch, E. Fron, J. Hofkens, Y. Mely, P. Naumov, M. Sliwa and P. Didier, *J. Phys. Chem. B*, 2015, **119**, 2638.
178 L. Yue, Z. Lan and Y.-J. Liu, *J. Phys. Chem. Lett.*, 2015, **6**, 540.